The R Coronae Borealis stars – atmospheres and abundances

M. Asplund[1,2], **B. Gustafsson**[2], **D.L. Lambert**[3,⋆], **and N.K. Rao**[4,⋆]

1 NORDITA, Blegdamsvej 17, 2100 Copenhagen Ø, Denmark
2 Astronomiska observatoriet, Box 515, 751 20 Uppsala, Sweden
3 Department of Astronomy, University of Texas, Austin, TX 78712, USA
4 Indian Institute of Astrophysics, Bangalore 560 034, India

Abstract. An abundance analysis of the H-deficient and He- and C-rich R Coronae Borealis (R CrB) stars has been undertaken to examine the ancestry of the stars. The investigation is based on high-resolution spectra and line-blanketed H-deficient model atmospheres. The models successfully reproduce the flux distributions and all spectral features, both molecular bands and high-excitation transitions, with one important exception, the C I lines. Since photoionization of C I dominates the continuous opacity, the line strengths of C I are essentially independent of the adopted carbon abundance and stellar parameters. All predicted C I lines are, however, much too strong compared with observations, with a discrepancy in abundance corresponding to 0.6 dex with little star-to-star scatter. Various solutions of this "carbon problem" have been investigated. A possible solution is that classical model atmospheres are far from adequate descriptions of supergiants such as the R CrB stars. We can also not exclude completely, however, the possibility that the gf-values for the C I lines are in error. This is supported by the fact that the C II, [C I] and C_2 lines are reproduced by the models with no apparent complications.

In spite of the carbon problem, various tests suggest that abundance ratios are little affected by the uncertainties. Judging by chemical composition, the R CrB stars can be divided into a homogeneous majority group and a diverse minority, which is characterized by extreme abundance ratios, in particular as regards Si/Fe and S/Fe. All stars show evidence of H- and He-burning in different episodes as well as mild s-process enhancements. Four of the majority members are Li-rich, while overabundances of Na, Al, Si and S are attributes of all stars. An anti-correlation found between the H and Fe abundances of H-deficient stars remains unexplained. These enigmatic stars are believed to be born-again giants, formed either through a final He-shell flash in a post-AGB star or through a merger of two white dwarfs. Owing to a lack of theoretical predictions of the resulting chemical compositions, identification of the majority and minority groups with the two scenarios is unfortunately only preliminary. Furthermore, Sakurai's object and V854 Cen exhibit aspects of both majority and minority groups, which may suggest that the division into two groups is too simplistic.

1. Introduction

This paper is concerned with the R Coronae Borealis (R CrB) stars and their putative progenitors and descendants. Our primary goal is to determine the chemical compositions of the R CrB stars and to use the results to sift evolutionary scenarios that purport to account for conversion of a H-rich star to one of these rare H-deficient stars.

Production of a He-rich luminous star demands an evolutionary history in which the following occur either alone, in tandem, or in concert: severe mass loss to remove most of the H-rich envelope of an evolved star; extensive deep mixing so that hydrogen is burnt to helium; mass transfer in a binary system that exposes the He-rich core. Of the evolutionary scenarios that have been sketched to account for R CrB stars (see the reviews by Renzini 1990; Schönberner 1996; Iben et al. 1996; Clayton 1996), two have been discussed extensively. In a scenario suggested by Webbink (1984), an R CrB star is the result of a merger of a C-O white dwarf and a He white dwarf; Iben et al. (1996) extend this scenario to include a merger of a neutron star with a white dwarf or a helium star to produce a Thorne-Żytkow (1975) object. In the second scenario (Fujimoto 1977; Renzini 1979), an R CrB star evolves from a post-AGB star which experiences a final thermal pulse when it descends the white dwarf cooling track. The pulse expands the envelope and the star is transformed to a red supergiant ('a born again AGB star') before quickly cooling and contracting once again into a white dwarf. The R CrB stars are generally viewed as intimately related to the non-variable hydrogen-deficient carbon (HdC) stars and the extreme helium (EHe) stars, but not to hydrogen-deficient binaries such as υ Sgr and KS Per (HD 30353) (Jeffery 1996).

Information about the chemical composition and the atmospheric structure is coded in the stellar spectrum, which can be

---

extracted using model atmospheres. Until recently, the only existing grid of model atmospheres for R CrB stars was that by Schönberner (1975) but the state of the art has developed since then. Therefore, we have constructed new models (Asplund et al. 1997a) which should be more representative of R CrB stars. In the present paper, these new models are tested for the first time in an extensive analysis; a test which – as will be seen – yields a most interesting and unexpected result with possible implications extending far beyond this particular class of peculiar stars.

Our spectroscopic survey of the R CrB stars was begun at a time when only three of the about 40 known examples had been subjected to quantitative analysis. Analyses of a large sample are needed to reveal the range in the chemical compositions, to make fair comparisons with putative progenitors and descendants, and to identify the 'unusual' R CrB stars that may be especially informative for constructing plausible evolutionary scenarios. In this paper, we analyse high resolution spectra of 17 R CrB stars and two 'cool' EHe stars with similar temperatures. The latter two may provide a link between the 'hot' EHe stars and the R CrB stars. Our sample includes most of the known galactic R CrB stars except the few hot and the several cool members. The analysis of V854 Cen was presented separately (Asplund et al. 1998), while we defer analysis of the coolest R CrB stars and the HdC stars to later papers. For hot R CrB stars and EHe stars, we cull results from the literature. Comparison will also be made with the recently identified born-again giant Sakurai's object, which shows similarities with the R CrB stars (Asplund et al. 1997b, 1999).

2. Observations

The stars studied here are listed in Table 1 together with the log of the different observing runs. Spectra were obtained when the stars were at or about maximum light (i.e. not during one of the defining visual declines of R CrB stars, but not necessarily close to the pulsational maximum), during three observing runs with the Cassegrain echelle spectrograph on the CTIO 4m reflector. In July, 1989, spectra were obtained in the red (5500–6800 Å) at a resolution of about 0.3 Å. Blue (4200–4900 Å) spectra at a resolution of 0.3 Å were also obtained for RT Nor, RS Tel, and RY Sgr. Spectra of a quartz halogen lamp were used to correct for the pixel-to-pixel variation of sensitivity and for the blaze profile of the echelle grating. Observing runs at CTIO in July, 1991, and May, 1992, provided spectra of the more northern R CrB stars and of additional southern stars. Several R CrB stars observed in 1989 were re-observed in 1992, in the interval 5480 to 7090 Å at a resolution of about 0.15 Å.

Spectra of XX Cam, SU Tau, and UV Cas were obtained in November and December, 1991, at the W. J. McDonald Observatory using the coudé spectrographs of the 2.1m and 2.7m reflectors, with a resolution of about 0.3 Å or better. Finally, the eponym, R CrB, is included in our analysis using the McDonald spectra analysed previously by Cottrell & Lambert (1982).

The reduced spectra were examined for lines for which the equivalent widths could be measured reliably. Except for three spectral regions (see below) spectrum synthesis was not attempted. About 100 to 200 lines per star were measured in total with an emphasis on lines of especial nucleosynthetic interest. Table 2, which is only available electronically through CDS, contains a complete line list for the individual stars with the adopted atomic parameters, measured equivalent widths and derived elemental abundances for the considered lines.

3. Abundance analysis – principles

3.1. Introduction

Our first abundance analysis (Lambert & Rao 1994) was made with the grid of non-blanketed models constructed by Schönberner (1975). The analysis was redone with the new line-blanketed models described in Asplund et al. (1997a) in the expectation that results would be more representative of the true chemical compositions.

At the outset, we clarify what is meant by 'abundance' in the context of the R CrB stars with their peculiar compositions. The strength of a (weak) line of an element E in a stellar spectrum is governed by the ratio of the line absorption coefficient (l_ν) to the continuous absorption coefficient (κ_ν). In the case of H-rich stars in the temperature domain of the R CrB stars, κ_ν in the visible spectrum is proportional to the number density of H atoms while l_ν is proportional to the number density of atoms E. Then, the line strength is controlled by the number density ratio E/H which is what is most often meant by the abundance of element E. As long as the He/H ratio is close to its normal value ($\simeq 0.1$), the abundance E/H may be expressed adequately as a mass fraction Z(E) without a precise determination of the He/H ratio, an unobservable quantity for cool stars. Mass fractions hold the clues to the history of the stellar atmosphere; for example, addition of CNO-cycled He-rich material will increase an atmosphere's E/H ratio but not change the mass fraction Z(E) of elements that do not participate in nuclear reactions at the low temperatures of CNO-cycling. Mass fractions can, however, be modified by chemical processes such as dust-gas separation which is discussed further in Sect. 6.1.2.

In the case of the R CrB stars, C I is thought to be the leading contributor to the continuous opacity in the line-forming layers across the interval spanned by our spectra (Asplund et al. 1997a). To convert the observed abundance S(E) = E/C to the more fundamental mass fraction Z(E), it is necessary to determine or to assume the C/He ratio, since He is likely to be the most abundant element. The mass fraction Z(E) may be written as

$$Z(E) = \frac{\mu_E E}{\mu_H H + \mu_{He} He + \mu_C C + ...} = \frac{\mu_E E}{\Sigma \mu_I I}, \tag{1}$$

where μ_I is the atomic mass of element I and the summation in the denominator includes all elements. This denominator is conserved through all the ravages of nuclear burning. Assuming He to be the dominant constituent, Eq. (1) may be recast in terms of the observable quantity S(E) and the C/He ratio ($\ll 1$) to give

$$Z(E) \simeq \frac{\mu_E}{\mu_{He}} \frac{C}{He} S(E). \tag{2}$$

Table 1. Log containing the observational details for the spectra obtained for the current project. The spectra of R CrB are taken from Cottrell & Lambert (1982).

Star	Date	Wavelength region [Å]	exp. time [min]	airmass	l	b	$v_{\rm rad}$ [km s^{-1}]	IS components[a] [km s^{-1}]
UX Ant	16/17 July 1989	5500–6800	2 x 30	1.24	279	20	132	-1, 21
	20/21 May 1992	5480–7090	45, 60	1.01	279	20	142	-1, 21
	21/22 May 1992	5480–7090	60	1.02	279	20	142	-1, 21
XX Cam	23–29 Dec 1991	5179–6790	[b]		150	1	16	
UV Cas	25–30 Dec 1991	5800–6790	[b]		110	0	-31	-50, -16
UW Cen	20/21 May 1992	5480–7090	20, 40	1.10	302	8	-41	
V CrA	16/17 July 1989	5500–6800	24, 2 x 30	1.10	358	-16	-10	9
	20/21 May 1992	5480–7090	60	1.01	358	-16	-10	9
	22/23 May 1992	5480–7090	60	1.19	358	-16	-10	9
V482 Cyg	20/21 May 1992	5480–7090	60	2.28	70	2	-41	-12
	21/22 May 1992	5480–7090	60	2.32	70	2	-41	-12
Y Mus	15/16 July 1989	5500–6800	3 x 8	1.25	304	-3	24	-21, 19
	21/22 May 1992	5480–7090	2 x 20	1.26	304	-3	37	-21, 19
RT Nor	15/16 July 1989	5500–6800	3 x 10	1.19	327	-7	-51	-4
	17/18 July 1989	4200–4900	2 x 30	1.16	327	-7	-51	-4
RZ Nor	15/16 July 1989	5500–6800	20, 30	1.10	332	-4	-70	-13
FH Sct	21/22 May 1992	5480–7090	2 x 60	1.10	24	-3	103	-14, -4, 28, 55, 77, 92[c]
GU Sgr	20/21 May 1992	5480–7090	2 x 40	1.10	8	-5	-39	-52?, -4, 10, 25
RY Sgr	16/17 July 1989	5500–6800	5 x 1	1.01	4	-19	-27	
	17/18 July 1989	4200–4900	3 x 10	1.01	4	-19	-27	
	22/23 May 1992	5480–7090	1, 2	1.00	4	-19	-14	
VZ Sgr	15/16 July 1989	5500–6800	10, 2 x 15	1.08	3	6	230	-151, -120, -8
V3795 Sgr	15/16 July 1989	5500–6800	3 x 20	1.01	6	-4	-30	-99
SU Tau	23–29 Dec 1991	5179–6790	[b]		189	-1	48	
RS Tel	16/17 July 1989	5500–6800	2 x 10	1.04	348	-14	-12	
	17/18 July 1989	4200–4900	2 x 30	1.04	348	-14	-12	
LS IV $-14°109$	22/23 May 1992	5480–7090	25, 45	1.10	21	-8	5	
BD $+1°4381$	20/21 May 1992	5480–7090	35	1.19	50	-25	12	

[a] Interstellar absorption components in Na I D lines
[b] In December, 1991, each order of the spectrum (≈ 50 Å) was taken separately with exposure times of typically 30–40 min.
[c] Located behind NGC 6694

A few additional prelusive remarks are in order. First, the strengths of the observed C I lines are insensitive to the C/He ratio, $T_{\rm eff}$ and $\log g$ (e.g. Schönberner 1975; Pollard et al. 1994). This insensitivity arises because the observed C I lines and the photoionization of C I that provides most of the continuous opacity originate from levels of similar excitation potential. This implies that weak C I lines will be of similar equivalent width from one star to the next, which is confirmed by observations (cf. Fig. 1 in Rao & Lambert 1996) and demonstrated by our calculations.

Second, in our sample there are stars with weaker than average lines of metals such as Fe. This does not imply that these stars are metal-poor in the sense that they have a lower than average mass fraction of Fe. The weak-lined stars may have higher C/He ratios but similar mass fraction of metals as other stars.

Third, the role of the C/He ratio is largely cancelled in considering abundance ratios, because from Eq. (2)

$$\frac{Z(E_1)}{Z(E_2)} = \frac{\mu_{E1}}{\mu_{E2}} \frac{S(E_1)}{S(E_2)}. \tag{3}$$

Therefore a dependence on the C/He ratio enters only through its (weak) influence on S(E) through its effect on the atmospheric structure and the fact that the lines of the elements E_1 and E_2 may be formed in different layers.

Fourth, the He I 5876 Å triplet is present in the spectra of almost all of our R CrB stars. Since this is a potential monitor of the C/He ratio, we discuss this line in detail later. In hotter H-deficient stars such as the EHe stars, the He I spectrum is well represented and a direct spectroscopic measurement of C/He is possible. Such measurements are a possible guide to the C/He ratios of the R CrB stars.

3.2. Model atmospheres

The analysis is based on new line-blanketed model atmospheres (Asplund et al. 1997a). Here only a recapitulation will be given; for details we refer to the original paper. The models are based on the usual assumptions: flux constant, plane-parallel layers in hydrostatic and local thermodynamic equilibrium (LTE). The models are calculated with an extended version of the original

MARCS code (Gustafsson et al. 1975), with special effort being made to include a complete inventory of continuous opacities for H-deficient compositions. Most of the data were taken from the Opacity Project (here OP; Seaton et al. (1994) and references therein). In particular, the most important known continuous opacity sources C I, He I, He$^-$ and electron scattering are all taken into account, together with many other minor contributors.

The most important difference compared with previous models is the inclusion of the significant line-blanketing. This is essential in order to simultaneously reproduce both the high excitation lines such as the He I triplet and molecular bands such as the C$_2$ Swan bands. Line absorption was taken into consideration using opacity sampling with data basically from R.L. Kurucz (private communication) with additions for the lighter elements from other sources. Absorption from a number of diatomic molecules was also considered using opacity distribution functions.

The abundances used for the model atmospheres on which this analysis is based are, except for a few test cases, those employed by Asplund et al. (1997a), i.e. abundances derived for R CrB stars by Lambert & Rao (1994) using Schönberner's (1975) non-blanketed models. The effects on the results of the analysis of the inconsistency between the input and the derived abundance ratios are, however, minor, as will be illustrated below.

3.3. Abundance analysis – method

3.3.1. Atomic and molecular data

The gf-values for the lines used in our LTE analysis were largely taken from a compilation kindly provided by R. E. Luck. In many cases, accurate laboratory experiments have given the gf-values. In other cases, an inverted solar analysis has been used. The gf-values of the C I lines are discussed below. The gf-values for Fe I and Fe II lines were taken from Lambert et al. (1996) or estimated according to their recipes.

Three spectral regions of special interest have been modelled with detailed synthetic spectroscopy: the C$_2$ Swan 0–1 bandhead around 5635 Å, the blended C II lines at 6578.05 Å and 6582.88 Å, and the He I D$_3$ line at 5875.6–5876.0 Å, which is blended with two C I lines. The C$_2$ band is present only in stars with $T_{\rm eff} \lesssim 7000$ K. The C II lines are only clearly seen in the spectra of the hottest stars in our sample, and for the cooler stars the D$_3$ feature is most probably dominated by C I.

Basic line data for the C$_2$ lines (5560–5640 Å) were obtained from a recent line list of R.A. Bell (Bell & Gustafsson 1989), assuming a solar ^{12}C/^{13}C value of 89. A dissociation energy of D$_0$ = 6.21 eV was adopted (Huber & Herzberg 1979). The C$_2$ lines were supplemented with additional atomic lines (R.L. Kurucz, private communication), partly using astrophysical gf-values.

The C II line region (6566–6593 Å) contains lines of C I, C II, Si I, Fe I, and Ni I, as well as a number of weaker atomic lines. The gf-values for the C I and C II lines were taken from OP. The gf-values of the C I lines were decreased by 0.6 dex in order to compensate for the fact that the predicted equivalent widths of C I lines are consistently too strong, see Sect. 4. The rest of the gf-values for the atomic lines were obtained by fits to the solar spectrum.

The data for the He I triplet was taken from Wiese et al. (1969). The line is blended with the C I lines at 5875.48 Å and 5875.86 Å, which previous analyses have overlooked. Hibbert et al. (1993) predicted the gf-values for intermediate-coupling for these weak C I transitions: $\log gf = -4.72$ and -4.28 respectively, which were similarly diminished by 0.6 dex.

In all synthetic-spectrum calculations the abundances and microturbulence parameters $\xi_{\rm turb}$ were those obtained in the analysis of the particular star, except for the C/He ratio which was kept to 1% except for a few test cases. All spectra were convolved with a Gaussian profile having a full width at half maximum corresponding to typically 10 km s^{-1}, which was found to give a good fit to unblended line profiles. This profile includes both the instrumental profile and macroturbulence.

3.3.2. Spectroscopic fundamental parameters

For each star the microturbulence parameter $\xi_{\rm turb}$ was adjusted until the derived abundances from the same species was independent of equivalent width. Lines of C I, Fe I, and Fe II were always used for these determinations and sometimes lines of Ca I, S I and other species added information. To within the errors of measurements, $\xi_{\rm turb}$ was the same for all species in a given star.

Imposition of ionization equilibrium of Mg I/II, Al I/II, Si I/II, S I/II, and Fe I/II provides loci in the $T_{\rm eff}$–$\log g$ plane. Fe was used for all stars but the other elements were generally measurable in both ionization stages only for the hotter stars. Dissociation equilibrium involving the C$_2$ Swan 0–1 band was used in an analogous sense. The strengths of the He I triplet with its C I blend and the C II 6578 and 6582 Å lines provide additional indicators. At first glance, the 5876 Å feature would appear to be primarily responsive to changes of $T_{\rm eff}$. Closer scrutiny shows that it provides a locus that parallels the loci from ionization and dissociation equilibria, reflecting the fact that the C I contribution to the continuous opacity decreases relative to the He I line absorption when gravity decreases, as a result of increased ionization of C. The sensitivity of the C II lines to $T_{\rm eff}$ and $\log g$ is similar to that of other indicators.

The various loci run almost parallel in the $T_{\rm eff}$–$\log g$ plane, as exemplified in Figs. 1 and 2. To resolve $T_{\rm eff}$ from $\log g$ it was necessary to find additional loci having distinctly different slopes. An excitation temperature is an obvious choice, but although Fe I and Fe II are quite well represented, the line selection proved inadequate for a sufficiently accurate determination of $T_{\rm eff}$. In a few cases, [O I] lines combined with O I lines served as a measure of $T_{\rm eff}$ with only a weak $\log g$ dependence.

In order to provide a locus of quite different slope, we combined assumed values of the bolometric magnitude ($M_{\rm bol}$) of R CrB stars and their mass ($\mathcal{M}$). This combination gives the familiar expression
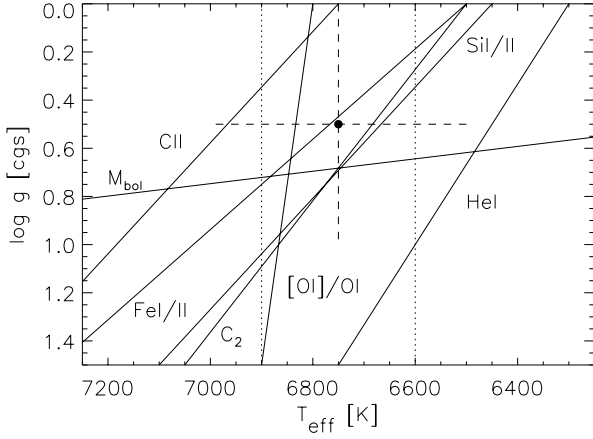
Fig. 1. The various loci provided by the T_{eff}-$\log g$ indicators for R CrB: ionization balance of Fe I/II and Si I/II, excitation balance of O I, line strengths of He I D_3, C II and C_2 0–1 Swan band, and estimate from bolometric magnitude. The dotted curves denote the interval of allowed T_{eff} estimates from the infrared flux method (Asplund et al. 1997a). Fitting the flux distribution in the visual and UV, and the $(B - V)_0$ photometry of the star also indicate T_{eff} in the same interval. The adopted parameters are marked with ●, and the estimated uncertainties are indicated by dashed lines. The estimate from the weak He I line would be shifted into better agreement with the other loci for this particular star if the C/He ratio had been 3% rather than the adopted 1%
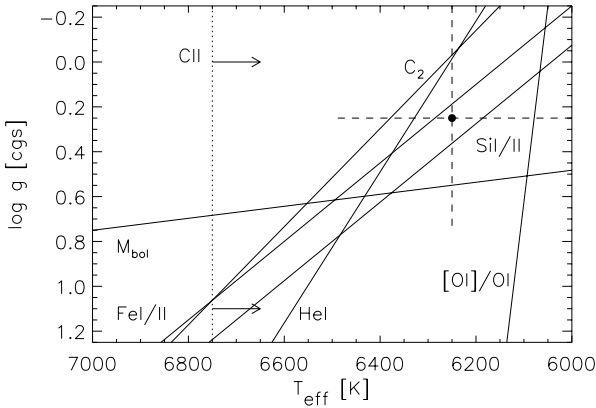

Fig. 2. Same as in Fig. 1 but for FH Sct. Lower weight has here been given to the excitation balance of O I because of the weak [O I] line.

$$\begin{aligned}
\log g &= \log g_\odot + 4\log\frac{T_{\mathrm{eff}}}{T_\odot} + \log\frac{\mathcal{M}}{\mathcal{M}_\odot} \\
&\quad + 0.4(M_{\mathrm{bol}} - M_{\mathrm{bol},\odot}) \\
&= -12.48 + 4\log T_{\mathrm{eff}} + \log\frac{\mathcal{M}}{\mathcal{M}_\odot} + 0.4M_{\mathrm{bol}} \quad (4)
\end{aligned}$$

The most reliable estimates of M_{bol} come from the R CrB stars in the Large Magellanic Cloud (LMC). Alcock et al. (1996) estimate M_{bol} for each of the now five known R CrB stars in the LMC, with values between -4.0 and -5.7. All of these estimates are subject to uncertainties arising from the distance modulus, reddening correction, and probably different metallicities as compared with galactic stars. We note that Glass et al. (1994) estimated $M_{\mathrm{bol}} \simeq -5.0$ for one of the stars for which Alcock et

Table 2. The analysed R CrB and EHe stars with their adopted stellar parameters. The estimated typical uncertainties are $\Delta T_{\mathrm{eff}} = \pm250\,\mathrm{K}$, $\Delta\log g = \pm0.5$ dex and $\Delta\xi_{\mathrm{turb}} = \pm1.0\,\mathrm{km\,s^{-1}}$.

Star	T_{eff} [K]	$\log g$ [cgs]	ξ_{turb} [km s^{-1}]
R CrB stars:			
V3795 Sgr	8000	1.00	10.0
UW Cen	7500	1.00	12.0
Y Mus	7250	0.75	10.0
XX Cam	7250	0.75	9.0
RY Sgr	7250	0.75	6.0
UV Cas	7250	0.50	7.0
RT Nor	7000	1.50	5.0
VZ Sgr	7000	0.50	8.0
UX Ant	7000	0.50	5.0
RS Tel	6750	1.25	8.0
RZ Nor	6750	0.75	7.0
R CrB	6750	0.50	7.0
V482 Cyg	6500	0.50	4.0
SU Tau	6500	0.50	7.0
V CrA	6250	0.50	7.0
GU Sgr	6250	0.50	7.0
FH Sct	6250	0.25	6.0
EHe stars:			
LS IV $-14°109$	9000	1.00	8.0
BD $+1°4381$	8500	1.50	8.0

al. find $M_{\mathrm{bol}} \simeq -5.7$. Estimates for the galactic objects R CrB and V482 Cyg have suggested $M_{\mathrm{bol}} \simeq -4.6$ (Rao et al. 1981; Rao & Lambert 1993). We adopt $M_{\mathrm{bol}} = -5\pm1$ for the present sample of warm R CrB stars. A mass $\mathcal{M}/\mathcal{M}_\odot = 0.7\pm0.2$ seems reasonable in light of the conjectures concerning their origins; for example, Weiss (1987) concludes from pulsation calculations that R CrB stars are stars of mass $0.8 < \mathcal{M}/\mathcal{M}_\odot < 0.9$, while Iben et al. (1996) suggest a slightly lower value from evolutionary considerations.

These values of M_{bol} and $\mathcal{M}$ yield the relation

$$\log g = -14.63^{+0.50}_{-0.55} + 4\log T_{\mathrm{eff}} \quad (5)$$

which intercepts the spectroscopic T_{eff}–$\log g$ loci at an adequate angle (Figs. 1 and 2). The estimated stellar parameters are listed in Table 2.

A check on the effective temperatures is provided by available data on flux distributions. Asplund et al. (1997a) show that the blanketed models provide a good fit to the dereddened fluxes of the eponymous star R CrB from the ultraviolet to the near-infrared with a model corresponding to $T_{\mathrm{eff}} = 6900\,\mathrm{K}$, $\log g = 0.5$ and C/He=1%. The fit is insensitive to the adopted $\log g$ but slightly dependent on the C/He ratio. Application of the infrared flux method also gives $T_{\mathrm{eff}} = 6600$–$6900\,\mathrm{K}$ when using the individual abundances of R CrB for the models; the uncertainty in the estimate of T_{eff} arises because of an IR excess compared with the theoretical fluxes (Asplund et al. 1997a). R CrB appears to be only slightly reddened so the corresponding uncertainties are probably small. Our spectroscopic tempera-

ture $T_{\rm eff} = 6750\,$K is consistent with these estimates, especially since Rao & Lambert (1997) find that $T_{\rm eff}$'s derived from maximum and minimum light of the semi-regular pulsations for this star differ by about 500 K. Dereddened colours could in principle be used to determine $T_{\rm eff}$ but unfortunately theoretical colours are not yet sufficiently accurate (Asplund et al. 1997a). Observed $(B-V)_0$ colours have, however, been used for a differential temperature ranking of the individual stars, which is consistent with the adopted stellar parameters.

The estimated $T_{\rm eff}$ for our two EHe stars are in reasonable agreement with the values quoted by Drilling et al. (1984) derived from UV photometry: $T_{\rm eff} = 9000\,$K for LS IV $-14°109$ and $10000\,$K for BD $+1°4381$, while our estimates are 9000 K and 8500 K, respectively.

The gratifying consistency between all the various $T_{\rm eff}$-$\log g$ indicators, molecular bands, high-excitation lines and flux distributions, for most stars is in sharp contrast to the case with models lacking line-blanketing, where the different indicators show very poor agreement. Though the adopted stellar parameters have undergone relatively minor revisions, this agreement indicates that the new model atmospheres are significantly more reliable, which naturally also carries over to the derived abundances. Certainly, line-blanketing must be included in order to infer realistic results, in particular in these H-deficient environments.

3.3.3. The C/He ratio

The 5876 Å feature offers a prospect of deriving the C/He ratio. Unfortunately, there are reasons why the feature is not an ideal abundance indicator. First, the C I contribution is appreciable for the cooler R CrB stars. Second, the He I contribution is sensitive to the adopted $T_{\rm eff}$ and $\log g$; for $T_{\rm eff} \simeq 7000\,$K, the equivalent width of the 5876 Å feature predicted for C/He=1% is matched by that for C/He=3% if $T_{\rm eff}$ is raised by $\simeq 500\,$K. Third and most importantly, the He I line with its high excitation potential is formed in the deepest photospheric layers, which means that it is highly saturated even when it appears relatively weak. The temperature sensitivity of the predicted 5876 Å feature is cancelled partially when combined with the C II lines for estimating the C/He ratio, which is possible for the hottest stars of the sample. Within the expected errors, a ratio of C/He=1% seems appropriate for the stars, though there is some indication that the ratio should be higher ($\sim 10\%$) for a few stars, most notably V3795 Sgr and VZ Sgr, which both belong to the so-called minority group (see below). Whether this may indicate two different evolutionary backgrounds will be discussed in Sect. 6.2.

If the hot EHe stars are indeed related to the R CrB stars, their C/He ratios provide a guide to the expected values in R CrB stars. The C/He ratio is directly obtainable in EHe stars from He I and C II lines. The previously analysed EHe stars have a mean C/He $= 0.76\% \pm 0.26\%$ with a total range of 0.30–1.0% (Jeffery 1996, 1998; Jeffery et al. 1998; Drilling et al. 1998), which suggests that C/He =1% is a reasonable choice. Jeffery (1996) also lists 3 unusual EHe stars with much lower C/He

ratios, ranging from 0.002% to 0.02%, which are not included in our comparisons with EHe stars.

In his analysis of three R CrB stars, Schönberner (1975) adopted C/He=3% but his study preceeded the analyses of the EHe stars and hence was not guided by their results.

4. The carbon problem

4.1. Definition

It has already been mentioned that since photoionization of C I is the dominant opacity source through most of the line-forming regions of R CrB stars, the equivalent widths of the C I lines are insensitive to C/He, $T_{\rm eff}$ and $\log g$. Thus, reliable predictions of weak C I equivalent widths should be possible despite quite large uncertainties in the defining parameters. However, the predicted equivalent widths exceed the observed values by a clear margin: a discrepancy which has been dubbed the 'carbon problem' (Gustafsson & Asplund 1996). It is important to emphasize that a new model constructed with the derived C abundance will *not* return its input abundance; the new model will have a carbon problem of a quite similar magnitude. Not until C/He is decreased significantly ($\lesssim 0.05\%$) such that C I no longer dominates the continuous opacity will a consistent C abundance be obtained in such an iterative procedure. Such a low ratio is, however, unacceptable for reasons discussed below.

The carbon problem is not a minor matter. The derived C abundances from 17 R CrB stars range from 8.6 to 9.2 for a mean of 8.88 with a dispersion of only 0.16, which should be compared with the input abundance of 9.52 for C/He=1%, i.e. a discrepancy of a factor of 4. The star-to-star spread is likely attributable to the errors of measurement which are dominated by the consequences of having few weak C I lines; 13 of the 17 stars have a derived abundance in the range 8.8 to 9.0. Our two EHe stars give C abundances of 8.6 (BD $+1°4381$) and 8.9 (LS IV -14°109), and the problem has also the same magnitude in V854 Cen (Asplund et al. 1998) and Sakurai's object (Asplund et al. 1997b, 1999). There is no obvious correlation of the problem with $T_{\rm eff}$, $\log g$, or $\xi_{\rm turb}$, but there is an indication of a inverse trend with the metallicity, as seen in Fig. 3. The correlation is, however, controlled in large part by the 'minority' R CrB stars whose compositions differ in distinct ways from other R CrB stars (see below). Their overall lower abundances may make the adopted model atmospheres less appropriate than for the other stars, which might cause an increased carbon problem. There is furthermore no obvious trend with wavelength of the C I lines, though the spectral coverage with lines in the interval 5 500 and 7 000 Å may be too limited to uncover such a trend, if present.

As expected, errors in $T_{\rm eff}$ and $\log g$ have a small effect on the carbon problem; for example, if alternative models are chosen for Y Mus that satisfy the ionization equilibria, extreme adjustments of $T_{\rm eff}$ by $\pm1000\,$K with simultaneous adjustments of $\log g$ by about ±1.0 dex result in changes of the C abundance of less than 0.1 dex. Even if ionization equilibria are discarded, implausible adjustments of $T_{\rm eff}$ and $\log g$ are required to remove the carbon problem.
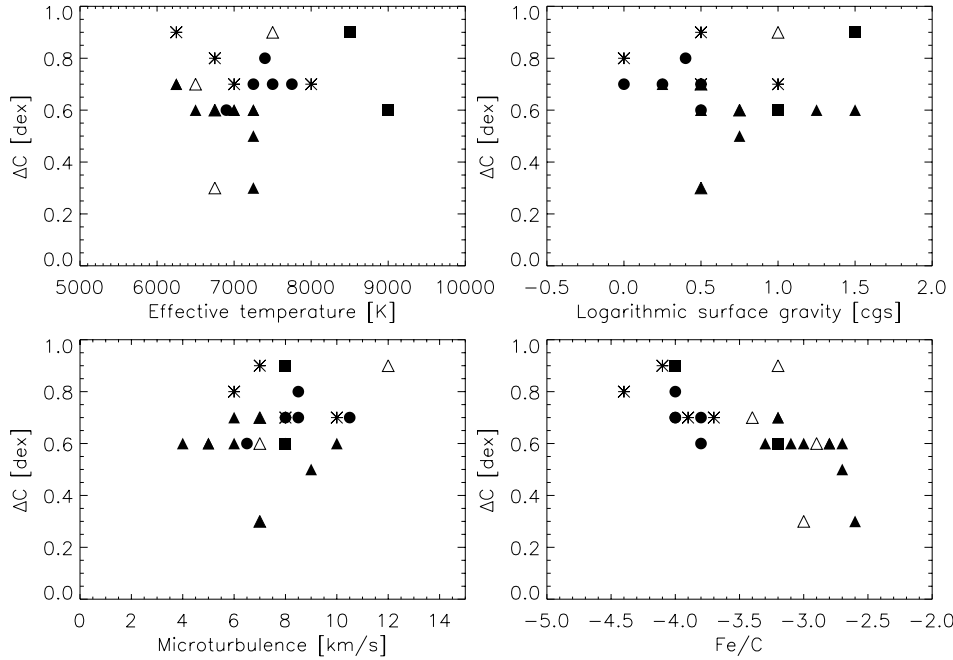
Fig. 3. The magnitude of the carbon problem ΔC for the analysed H-deficient stars, i.e. the input C abundance relative to derived spectroscopic abundance. The symbols refer to: Li-rich majority stars ($\triangle$), other majority members (black triangles), minority R CrB stars ($*$) (including V854 Cen, Asplund et al. 1998), our two EHe stars (black squares) and Sakurai's object ($\bullet$) in April, May, June, July and October 1996 (Asplund et al. 1999). Note that in some cases different stars overlap each other

Most of the C I lines used are sensitive to the adopted $\xi_{\rm turb}$, and an inappropriately chosen $\xi_{\rm turb}$ could therefore lead to erroneous C abundances. However, the C I lines indicate similar $\xi_{\rm turb}$ as compared with lines of other species. Furthermore, the discrepant weak C I lines, which show the same carbon problem as the strong lines, cannot be explained by changing $\xi_{\rm turb}$.

The question arises whether the C II lines also exhibit the carbon problem. These lines, although blended, are of useful strength in the hottest stars. For V3795 Sgr, UW Cen, and RY Sgr, the C II lines can not be explained if their *gf*-values differ by more than 0.2 dex from the true values, even when possible errors in $T_{\rm eff}$ and g are considered. This is an indication that the carbon problem applies to C I but not to C II. Due to the carbon problem, ionization balance for C is not fulfilled, while it is achieved for elements such as Fe and Si for the adopted parameters.

The astonishing result that all stars analysed return a carbon problem of about 0.6 dex, raised natural worries that there might be an error in the implementation of the methods, e.g. a programming error. In addition to systematic debugging we have made independent checks of this possibility. The existence of the carbon problem has been independently verified with completely different H-deficient models and synthetic spectrum codes (N. Piskunov & Y. Pavlenko, private communication) and in independent studies (Kipper & Klochkova 1997; Vanture et al. 1999). We consider a simple programming error unlikely. We note that the earlier abundance analysis with Schönberner's non-blanketed models (Lambert & Rao 1994) led to a considerably smaller carbon problem of about 0.2 dex, which is reproduced with non-blanketed models calculated by us. We ascribe this result mainly to the different temperature gradients; the flatter temperature gradient of the non-blanketed models results in weaker C I lines. (Naturally, this does not mean that one should go back to more primitive non-blanketed models with their more

shallow gradients – the effects due to blanketing are there in the physical world.) Also, the generally smaller κ_ν for given T and $P_{\rm e}$ in our models compared with the data adopted by Schönberner tends to make the C I lines stronger. The problem has also been verified with the analytical method of weighting functions for the calculation of equivalent widths of weak lines (cf. Unsöld 1955).

4.2. Possible solutions

A resolution of the carbon problem has been sought among the following diverse hypotheses:

1. The measured equivalent widths underestimate the true equivalent widths of the photospheric spectrum.
2. The basic atomic data for C I are in error.
3. Photoionization of C I is not the dominant contributor to the continuous opacity
4. The assumption of LTE for C I is invalid.
5. The adopted model atmospheres are inappropriate.

4.2.1. Equivalent widths and non-photospheric emission

The carbon problem would be alleviated if the photospheric equivalent widths were diminished by non-photospheric emission, but the adjustments required are great. For all stars, we have measured some (apparently) weak C I lines and the required change of equivalent width for these is close to the full 0.6 dex. A simple measurement error of this magnitude is ruled out: in these warm R CrB stars the continuum is well defined and blends are rarely much of a problem. Any postulated extra-photospheric continuous flux must be of the order of 3 times the photospheric flux across the observed wavelength interval. That would put strong demands as regard extra energy resources, and

the good fit between the calculated and observed flux curve for R CrB would require the flux to be spread over a considerable part of the spectrum.

Although a circumstellar dust shell is a common feature of R CrB stars, it seems improbable that emission by this shell is the dominant flux contributor in the optical. Seemingly incompatible observational facts are that (i) the magnitude of the carbon problem is essentially uniform across the sample but (ii) the infrared excesses vary considerably (Walker 1986). The existence of such a dust shell is difficult to defend also on theoretical grounds, since the dust temperature hardly can exceed $\simeq 2500$ K. An optically thick shell at this temperature can be excluded due to the lack of a very substantial near-infrared excess. Conceivably, the product $\kappa_\lambda B_\lambda(T)$, which controls the emitted flux for an optically thin shell, might be engineered to put maximum flux in the observed wavelength interval but the energy requirements still seem extraordinarily severe.

A high-density chromospheric-like region is certainly an observed attribute of the R CrB stars (cf. Clayton 1996). To provide the required additional flux from free-bound C I emission, a chromosphere with a volume emission measure of $\approx 2 \cdot 10^{62}$ cm^{-3} (e.g. a region extending from the surface to 2 stellar radii with $N_e \simeq 2 \cdot 10^{11}$ cm^{-3}) with a temperature of 7000 K is needed. For V854 Cen, Clayton et al. (1992) estimate a volume emission measure of only 10^{58} cm^{-3} from the observed emission lines during a decline. Possibly, this emission may be unrepresentative of an inner bright chromosphere which is presumably occulted at minimum light, but the required emission measure seems yet excessively large.

Electron scattering may make all lines seemingly weaker by Doppler shifting continuum photons into the lines due to the large thermal velocities of the electrons. The electron scattering optical depth τ_e in the model atmospheres outside the C I line-forming region is, however, too small for this partial redistribution to be effective, according to estimates following Mihalas (1978). Additional electrons must therefore be postulated; the chromosphere sketched above will have $\tau_e \simeq 0.8$ and thus distort the lines significantly.

The substantial corrections to the strengths of relatively strong lines from additional continuous flux would, however, imply very high ξ_{turb} ($\gtrsim 25$ km s^{-1}), far beyond the photospheric sound velocities ($\simeq 5$ km s^{-1}). Moreover, the photospheric He I, C II and C$_2$ lines would in reality then be stronger than observed, and thereby the difficulty of fitting spectral features of different excitation would be increased.

Ultraviolet emission lines are present at maximum light, and in the optical the strongest low excitation lines of singly-ionized ions appear distorted by emission (Lambert et al. 1990). These and other emission lines appear a couple of magnitudes below maximum during a decline, but none of the observed C I lines go into emission (Alexander et al. 1972). This suggests that line emission is not the solution to the problem. To resolve the problem the chromosphere must for all stars fill in the C I lines with emission at maximum by the same amount yet not introduce observable line emission for any line nor during the

early phases of a decline. We consider this a rather contrived explanation.

Though not completely ruled out, non-photospheric emission weakening the C I lines seems to be an unlikely solution.

4.2.2. Basic atomic data for neutral carbon

The adopted *gf*-values for C I were taken from the OP calculations (Seaton et al. 1994; Luo & Pradhan 1989) and the assumption of LS-coupling. An alternative choice for *gf*-values would be the compilation of semi-empirical calculations including intermediate coupling by Kurucz & Peytremann (1975, here KP). Calculations with intermediate coupling have been given by Hibbert et al. (1993) for a few multiplets. When overlap exists, the latter source agrees well with the OP values.

Inspection of OP and KP *gf*-values shows that exclusive use of the latter would reduce the carbon problem but the line to line scatter of the abundances would be increased significantly. For example, the carbon abundance for Y Mus from 8 lines weaker than 170 mÅ, is increased by 0.37 dex when KP *gf*-values are used but the dispersion is increased from 0.19 dex, a value consistent with errors of measurement, to 0.56 dex.

In three of the analysed stars (R CrB, XX Cam and Sakurai's object) the spectra cover the forbidden [C I] line at 9850.2 Å. It is noteworthy that the carbon problem seems not to exist for this line: in all three stars [C I] returns a carbon abundance 0.0–0.2 dex *higher* than the input abundance. Naturally, this could also be due to erroneous stellar parameters or atmospheric temperature structures, since the [C I] line is more sensitive to the temperature than the C I lines. However, it would require rather large errors in T_{eff} for the two types of lines to return the same abundance, typically ~ 750 K. It should be noted also that for the currently adopted parameters the excitation balance of O I/[O I] is more or less satisfied. This may point to the conclusion that the carbon problem only applies to permitted carbon lines but not the forbidden lines, and thus possibly question the adopted *gf*-values. However, the evidence is still scarce and we are therefore hesitant to draw such a strong conclusion here, but certainly emphasize the need to further studies of the forbidden lines in more R CrB stars, as well as new independent determinations of the gf-values for the C I lines.

Cross-sections for photoionization of C I were also taken from OP. At the shortest wavelengths considered, the excitation potentials of the contributing levels are $\chi \gtrsim 9.2$ eV and correspond to principal quantum numbers $n \gtrsim 3$, while the measured lines come from levels with $\chi \simeq 8.5$–9.2 eV. Photoionization cross-sections influence the predicted C I equivalent widths in two ways: the total opacity influences the atmospheric structure, and the opacity at the wavelengths of the measured lines directly affects the equivalent widths. To obtain a consistent C abundance, one has to multiply the continuous opacity of C I by a factor of $\simeq 3$ across the interval from 5500 Å to 7000 Å where the lines are situated. Such an increase is, however, in conflict with the observed fluxes of R CrB (Asplund et al. 1997a); a more general multiplication across the spectrum would lead to smaller effects on the flux distribution but would demand a

greater increase (factor of $\simeq 5$) in order to eliminate the carbon problem.

The errors quoted by Seaton et al. (1994) as typical for both *gf*-values and photoionization cross sections in the OP data are 10%. For C I, the OP photoionization data agree reasonably well with those calculated by Peach (1970); typically the OP data are lower by 10–30% for relevant temperatures and wavelengths. An error of such a magnitude is far from what is needed. In our calculation of absorption coefficients from the OP data the resonances have been smoothed and only contributions from $n \lesssim 10$ have been included. The errors due to these simplifications should, however, not be serious.

In view of the error estimates in the OP data, it does not seem probable that errors in atomic data for carbon can resolve the problem. However, the absence of a corresponding C II problem and the probable consistency also for [C I] suggest that independent determinations of the gf-values for the C I lines should be made.

4.2.3. Missing opacity?

Unless C/He is much lower than 1%, C I is expected to be the dominant continuous opacity source. If the dominant continuous opacity is in fact not contributed by C – directly or indirectly – the carbon problem might be eliminated.

Other opacity sources but carbon that are known to contribute are so weak that it is highly improbable that errors in data for them could resolve the carbon problem. Any additional opacity not yet included must dominate across the ranges of T_{eff}, $\log g$ and composition spanned by our stars; a large variation of the additional opacity relative to the photoionization of C I would introduce large variations in the equivalent width of a given C I line, in conflict with the uniformity of the carbon problem. As noted earlier, the carbon problem seems not to be dependent on wavelength. No source of continuous opacity of this strength and uniformity is available, as far as we can see.

Furthermore, a neglected veil of lines is an unlikely possibility; although the carbon problem is of uniform magnitude for all stars the density of lines in their spectra varies considerably. It is also difficult to imagine what could contribute a veil. For example, a veil of molecular lines will not account for the carbon problem, since such lines are formed outside the C I line-forming region. Line blanketing has been included on the assumption that the lines are formed by pure absorption. However, even with a pure scattering contribution, the significant backwarming, and hence the carbon problem, remains.

In conclusion, we are not aware of any missing opacity source that could resolve the carbon problem.

4.2.4. A low C/He ratio?

Our preference for a C/He ratio of 1% is based on the EHe stars for which the C/He is directly determinable, and from the strengths of the He I and C II lines for our hotter stars. Conclusions about composition may also be drawn from the fact that the C I lines are similar from star to star. As C/He is reduced, other sources of opacity make a more effective contribution and the carbon problem is diminished. At a particular value of the C/He ratio, the carbon problem vanishes. Then, the observation that a C I line has a similar strength across the sample implies that all stars have a similar low C/He ratio. The required ratio is very low: C/He $\lesssim 0.05\%$, but such a low ratio is only found in three of the EHe stars (Jeffery 1996). More significantly, the C/He ratio derived for our hottest stars is inconsistent with such a low C/He ratio.

As part of the tests on the sensitivity of the derived abundances, one star (UX Ant) has been reanalysed using a consistently low C abundance (C/He=0.04%). The stellar parameters remain the same, though with slightly poorer agreement between the different indicators. The predicted C II lines are, however, much too weak compared with observations; i.e. one faces an as severe inverse carbon problem instead.

We conclude that the low C/He ratios needed to avoid the carbon problem are not acceptable.

4.2.5. Non-LTE effects

Non-LTE effects deserve consideration as a possible explanation for the carbon problem. Statistical equilibrium calculations using extensive model atoms show that the non-LTE effects are very small in the deep layers that produce the observed C I lines (Asplund & Ryde 1996). The derived abundances are affected typically by ± 0.02 dex for a representative model with $T_{\mathrm{eff}} = 7000$ K and $\log g = 0.5$. For the solar case the calculations of Asplund & Ryde (1996) agreed well with small non-LTE corrections found by of Stürenburg & Holweger (1990)

The small non-LTE effects are not unexpected. The lines are formed at great depths where the radiation field is close to isotropic and Planckian. The transitions are between highly excited levels with similar departures in their populations from the Boltzmann distribution. In addition, the strong line-blocking prevents significant overionization of carbon. Non-LTE effects, relative to those in normal H-rich supergiants, are probably smaller also due to the higher densities in the R CrB atmospheres.

The statistical equilibrium calculations were not fully self-consistent in the sense that the departures from LTE were not introduced into the calculation of the model atmospheres. Since the non-LTE effects are very small, we expect effects on the atmospheres in the line-forming region to be minor. Furthermore, carbon is *the* atom that controls the atmosphere as regards both opacity and electron density, and the non-LTE effects of C I are those that could affect the atmospheric structure significantly. It seems unlikely that consistent non-LTE model atmospheres will differ greatly from our present LTE models. The uniformity of the carbon problem with no obvious trends with either wavelength or multiplet membership, supports the interpretation of only minor departures from LTE.

In conclusion, we find that departures from LTE for C are most probably not responsible for the carbon problem.

4.2.6. The model atmospheres

The model atmospheres are built upon a set of assumptions that may not be valid for real R CrB stars. The effects of relaxing the assumption of LTE were discussed above.

Sphericity. R CrB model atmospheres are not very extended although they represent supergiants: typically the atmospheric thickness is 2–5% of the stellar radius for our plane-parallel models. To test the effect of extended atmospheres, we have calculated similar spherical models (Plez et al. 1992; Asplund et al. 1997a) though without line-blanketing. The effects on the C I lines are, however, very minor, since they are formed at great depths. Also, the slightly lower temperatures in the line-forming region compensate the slight increase in extension. Sphericity is obviously not a way to resolve the carbon problem.

Departures from hydrostatic equilibrium Turbulent pressure has not been included in the standard models, but tests show that the carbon problem can not be explained by this neglect. Its effect is similar to a gravity effect (Gustafsson et al. 1975) but the carbon problem is insensitive to gravity changes as shown above. For the same reasons, pulsations and mass loss are unlikely solutions. Furthermore, the stars have been observed at different pulsation phases but still show the same magnitude of the carbon problem, as is also illustrated by Rao & Lambert (1997) for R CrB.

Inhomogeneities. Since the estimated micro- and macroturbulent velocities exceed the sound velocity, the atmosphere is likely to be highly inhomogeneous. Effects of inhomogeneities on the predicted line spectrum are difficult to assess. However, the similar sensitivities of the C I line and continuous opacity to temperature and pressure fluctuations may suggest that inhomogeneities cannot explain the carbon problem.

Errors in model atmosphere structures. The weak observed C I lines might reflect a flatter than predicted photospheric temperature gradient. Deep layers ($\tau \geq 10$) are convectively unstable and the mixing-length theory is applied there. Although considerable convective overshoot is needed to affect the temperature gradient in the C I line-forming layers, our treatment of convection may be a contributor to an incorrect temperature gradient. More speculative, but perhaps more serious, are consequences of the super-Eddington luminosities in the same deep layers (Asplund & Gustafsson 1996; Asplund et al. 1997a; Asplund 1998).

In quantifying the effects of temperature-structure changes, we have been guided by the need for both a shallower temperature gradient in the C I forming region and the need to keep the steep overall temperature gradient in order to conserve as much as possible of the agreement with C_2, C II and He I lines as well as the agreement between observed and calculated fluxes
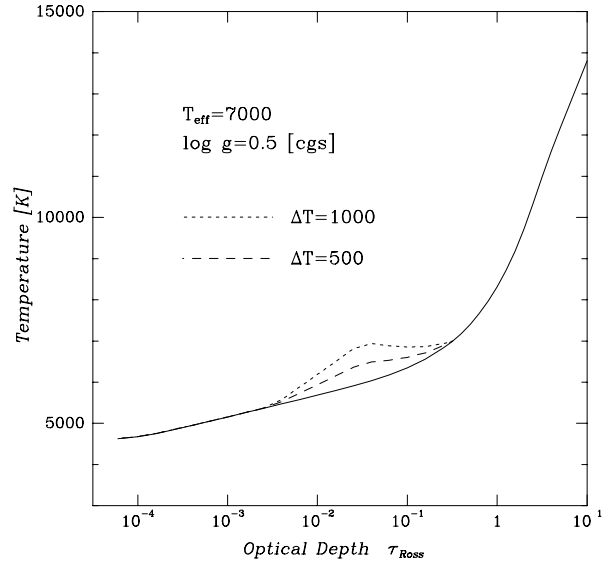

Fig. 4. The effect on the $T(\tau)$-relation of a typical model atmosphere when heating the C I line-forming region in order to eliminate the carbon problem. Two such adjusted models with maximum heating of 500 (dashed) and 1000 K (dotted) respectively are shown for a model with $T_{\text{eff}} = 7000$ and $\log g = 0.5$. The less extreme model still shows a carbon problem of about 0.3 dex

for R CrB. We have introduced a temperature correction to the standard models $T_0(\tau)$ of the form

$$T(\tau) = T_0(\tau) + \Delta T(\tau) \tag{6}$$

where

$$\Delta T(\tau) = \begin{cases} a(\log \tau - b_1) & ; \quad b_1 \leq \log \tau \leq (b_1 + b_2)/2 \\ a(b_2 - \log \tau) & ; \quad (b_1 + b_2)/2 \leq \log \tau \leq b_2. \end{cases} \tag{7}$$

Various combinations of the parameters a, b_1 and b_2 have been attempted, for which the equation of hydrostatic equilibrium was integrated and the continuous absorption coefficients calculated. The required heating parameter a to reproduce the C I lines is significant: $\simeq 1\,000$ K for $T_{\text{eff}} = 7\,000$. The optimum location of the heating is the same for most models ($\log \tau = -2.5$ to -0.5 with maximum heating at $\log \tau = -1.5$) which reflects the constant line strength and formation depth, independent of the stellar parameters, of the C I lines. As seen in Fig. 4 the revised temperature profiles are essentially flat in the interval $-1.5 \leq \log \tau \leq -0.5$.

Such drastic changes will affect the abundance analysis. The microturbulence parameters, as derived from the strengths of Fe I lines and C I lines come out practically unchanged. The ionization equilibria are also only marginally affected, but the consistency for the other T_{eff}-$\log g$ indicators is not fully preserved. The He I lines weaken due to the flatter temperature gradients, and in order to reproduce them an increase of T_{eff} of typically 200 K is needed at a given $\log g$. The corresponding increase necessary for C II is about 500 K, while the weakened C_2 bands suggest a decrease in T_{eff} of about 200 K. These changes thus increase the scatter between the different $T_{\text{eff}} - \log g$ indicators. Furthermore, the [C I] lines are also affected by the

postulated heating to such a degree that the discrepancy between the forbidden and permitted carbon lines as discussed in Sect. 4.2.2 largely remains the same.

These experiments establish the required temperature changes to resolve the carbon problem. Considering the very significant amount of heating, it should be questioned whether it is at all energetically reasonable. The extra flux ΔF radiated away from the heated region may be estimated to $\Delta F = 4\pi\kappa_P\rho\sigma(4T^3\Delta T)s$, where κ_P is the Planck mean opacity per gram, ρ the density, σ the Stefan-Boltzmann radiation constant, T the temperature and s the geometrical thickness of the heated region. The fraction of the total stellar flux that has to be used for this extra heating is on the order of 10%. For comparison, the chromospheric-coronal heating of late-type stars is limited to about 1% of the total bolometric flux.

Thus, the proposed heating needs a very efficient mechanism. It is in this respect interesting to compare with the total available mechanical flux $F_{\mathrm{mech}} = \beta v_{\mathrm{turb}}^3\rho$, where v_{turb} is the characteristic turbulent velocity, and β is a constant of order unity. If all this flux is heating the relevant layers one may estimate the resulting temperature increase there by equating F_{mech} and ΔF. In order to obtain $\Delta T \simeq 500\,\mathrm{K}$, velocities of typically $40\,\mathrm{km\,s^{-1}}$ are required. Such velocities well exceed the estimated sound and macroturbulent velocities. Moreover, the entire mechanical flux must be deposited in the photosphere.

4.3. Summary

It is clear that the virtue of the present blanketed models to reproduce the different diagnostics with a wide range of excitation (from C_2 to He I) is partly compromised when attempts are made to alleviate the carbon problem by decreasing the temperature gradient. For the moment disregarding from the possibility that the C I gf-values could be in error, we conclude that the R CrB spectra indicate that the basic assumptions of the standard model atmospheres (homogeneous, flux constant layers in hydrostatic equilibrium and LTE) are not valid. In this respect it is tantalizing that the carbon problem is significantly reduced during the early phases of a decline (Rao et al. 1999). It is important to realize that the reason why this verdict may be stated is not necessarily the peculiar character of these stars as such, except in one important respect: the basic control of the atmosphere by one atom, carbon, and even more specifically, its highly excited states. This, in fact, makes the R CrB stars excellent testing objects for standard model atmospheres. It is noteworthy that the result of this test is negative. A similar problem hampering the R CrB star analysis may thus also afflict H-rich supergiants, though it would be less obviously detectable. However, there are indications that the carbon problem only applies to the permitted lines of neutral carbon. It would therefore be worthwhile to ensure that the gf-values are in fact not to blame by new, independent determinations of the transition probabilities between these highly excited levels. The uniformity of the carbon problem would have a natural explanation if the transition probabilities are the culprits.

5. Abundance analysis – results

The derived stellar abundances are given in Table 3. Lambert & Rao (1994) have identified two groups of R CrB stars according to the observed (spectroscopic) metallicities. Most of the objects seem to form a homogeneous sample but a few stand out with their in general low abundances and peculiar abundance ratios, in particular Si/Fe and S/Fe. Of the stars analysed here V CrA, VZ Sgr and V3795 Sgr belong to the minority group, but also DY Cen (Jeffery & Heber 1993), and possibly V854 Cen (Asplund et al. 1998), Sakurai's object (Asplund et al. 1999) and a couple of EHe stars fall in this category. The two groups may indicate two different evolutionary backgrounds of these H-deficient stars. Before sifting the abundances for clues to the evolution of the stars, sources of uncertainty must be given a careful discussion, especially in light of the carbon problem.

5.1. Uncertainties in derived abundances

5.1.1. Statistical abundance errors

In Table 3, the statistical errors determined as the formal standard deviations for the different lines of an element are given; for elements with only a single line no error is given. Typically the statistical errors are on the order of 0.2 dex, though for some elements in some stars the errors are larger (0.3–0.5 dex). Na, Si, Sc and Ni normally have the smallest errors (typically 0.1 dex). Certain elemental abundance determinations rely only on a single line (e.g. H, Li and Zn, but also often Mg, Al, Ti, Zr and La) for which the statistical errors are hard to estimate. It should also be noted that in some cases the abundance have been derived from rather few lines, and thus the statistical errors may have been underestimated. More uncertain abundance determinations have in general been left out of Table 3.

5.1.2. Effects of line-blanketing

Lambert & Rao (1994) summarize abundances derived from non-blanketed models corresponding to a C/He ratio of 3%. In this case, the carbon problem was small (0.2 dex) such that it might be attributed to a combination of likely errors. The Fe abundance on the normal scale was $\log\epsilon(\mathrm{Fe}) = 7.5$ for the majority, or equivalent to a solar mass fraction $Z(\mathrm{Fe}) = 10^{-2.9}$ for the assumed C/He=3%. With blanketed models and C/He=1%, we derive $\log\epsilon(\mathrm{Fe}) = 6.5$ or $Z(\mathrm{Fe}) = 10^{-3.9}$. If instead the spectroscopic C abundances are adopted, the mass fractions from Eq. (2) are $Z(\mathrm{Fe}) = 10^{-2.7}$ and $10^{-3.3}$ for the non-blanketed and blanketed models, respectively, which reflects the different magnitude of the carbon problem for the two sets of models. The difference of 0.6 dex between these second estimates of $Z(\mathrm{Fe})$ is essentially that expected from the use of different C/He ratios.

Abundance ratios X/Fe are rather insensitive to the choice of non-blanketed or blanketed models. For elements from N to Ni, the difference in X/Fe is within ±0.1 dex in spite of differences in T_{eff}, $\log g$, ξ_{turb} and C/He. The Y/Fe and Ba/Fe ratios show larger changes (0.4 and 0.7 dex, respectively) when introducing line-blanketing; a part of this difference is attributable

Table 3. The individual elemental abundances for the analysed RCB and EHe stars. Abundances for V854 Cen are taken from Asplund et al. (1998) to allow easy comparison

	UX Ant	XX Cam	UV Cas	UW Cen	V CrA	R CrB	V482 Cyg	Y Mus	RT Nor	RZ Nor
H	6.9	< 4.1	6.0	6.5	8.0	6.9	4.8	6.1	6.5	5.2
Li	< 2.5	< 1.5	< 1.9	3.5	< 1.0	2.8	< 1.1	< 2.1	< 1.5	3.5
C[a]	8.9 ± 0.3	9.0 ± 0.4	9.2 ± 0.4	8.6 ± 0.3	8.6 ± 0.2	9.2 ± 0.2	8.9 ± 0.2	8.9 ± 0.4	8.9 ± 0.2	8.9 ± 0.3
N	8.3 ± 0.4	8.9 ± 0.3	8.5 ± 0.3	8.3 ± 0.4	8.6 ± 0.4	8.4 ± 0.2	8.8 ± 0.5	8.8 ± 0.3	9.1 ± 0.3	8.7 ± 0.4
O	8.8 ± 0.2	8.4 ± 0.1	7.5 ± 0.1	7.7 ± 0.2	8.7	9.0 ± 0.2	8.1 ± 0.3	7.7	8.4 ± 0.4	8.9 ± 0.1
Ne								8.3 ± 0.1		
Na	5.8 ± 0.1		6.4	6.0 ± 0.1	5.9 ± 0.2	6.1 ± 0.1	6.3 ± 0.1	6.3 ± 0.2	6.3	6.4 ± 0.3
Mg		6.8			6.6			6.3 ± 0.2		
Al			6.0	6.3 ± 0.2	5.3	5.8	6.2	6.1	6.2	6.3
Si	6.9 ± 0.3	7.1 ± 0.3	7.4 ± 0.2	7.0 ± 0.2	7.6 ± 0.1	7.2 ± 0.2	7.2 ± 0.1	7.3 ± 0.2	7.4 ± 0.4	7.1 ± 0.1
P								5.9 ± 0.2		
S	6.2 ± 0.0	6.8 ± 0.2	7.0 ± 0.1	6.7 ± 0.1	7.5 ± 0.3	6.8 ± 0.0	6.9 ± 0.3	6.9 ± 0.1	7.7 ± 0.2	6.8 ± 0.1
Ca	5.5 ± 0.2	5.4	5.6 ± 0.3	5.2 ± 0.2	5.1 ± 0.4	5.3 ± 0.3	5.4 ± 0.3	5.3 ± 0.3	5.8 ± 0.5	5.4 ± 0.5
Sc		2.8 ± 0.1		2.6 ± 0.1	2.8			2.8 ± 0.3		
Ti		4.0 ± 0.1	4.0	4.1 ± 0.1	3.3			4.2 ± 0.3		
Fe	6.2 ± 0.2	6.8 ± 0.2	6.9 ± 0.2	6.3 ± 0.2	5.5 ± 0.4	6.5 ± 0.1	6.7 ± 0.3	6.5 ± 0.3	6.8 ± 0.3	6.6 ± 0.2
Ni	5.8 ± 0.1	6.1 ± 0.1	6.2	5.9 ± 0.3	5.6	5.5 ± 0.1	5.8 ± 0.2	6.0 ± 0.3	6.2 ± 0.3	5.9 ± 0.2
Zn			4.8	4.3	2.9		4.4	4.4	4.7	4.4
Y	1.5 ± 0.2	2.0 ± 0.3	2.8	1.5 ± 0.1	0.6	1.5	2.6	2.4 ± 0.3	3.1	2.0 ± 0.2
Zr				1.8			2.3	2.6 ± 0.3	1.8	
Ba	1.0 ± 0.1	1.5	2.1	1.6 ± 0.1	0.7	1.6 ± 0.5	2.6 ± 0.2	1.5 ± 0.2	2.0 ± 0.1	1.5 ± 0.1
La			1.5	1.5			2.2	1.3 ± 0.3	1.9	1.1

	FH Sct	GU Sgr	RY Sgr	VZ Sgr	V3795 Sgr	SU Tau	RS Tel	LS IV −14°109	BD 1°4381	V854 Cen
H	5.6		6.9	6.2	< 4.1	7.4	6.5	6.1	6.2	9.9 ± 0.1
Li	< 1.0	< 1.1	< 1.8	< 1.5		2.6	< 1.4	< 2.8	< 3.0	< 2.0
C[a]	8.8 ± 0.3	8.8 ± 0.3	8.9 ± 0.2	8.8 ± 0.3	8.8 ± 0.2	8.8 ± 0.2	8.9 ± 0.3	8.9 ± 0.3	8.6 ± 0.2	9.6 ± 0.3
N	8.7 ± 0.2	8.7 ± 0.5	8.5 ± 0.2	7.6 ± 0.2	8.0 ± 0.3	8.5 ± 0.1	8.8 ± 0.2	8.6 ± 0.4	7.2 ± 0.3	7.8 ± 0.1
O	7.7 ± 0.2	8.2	7.9 ± 0.2	8.7 ± 0.1	7.5 ± 0.2	8.4 ± 0.3	8.3 ± 0.1		8.4 ± 0.1	8.9 ± 0.1
Ne					7.9 ± 0.3			8.9 ± 0.2	8.1 ± 0.2	
Na	6.1 ± 0.2	6.0 ± 0.1	6.3 ± 0.1	5.8 ± 0.1	5.9 ± 0.1	5.6 ± 0.1	6.0 ± 0.1	6.4 ± 0.1	5.4	6.4 ± 0.1
Mg		6.9			6.1 ± 0.2			7.0	6.1	6.2
Al	5.9	5.7	6.0	5.4	5.6 ± 0.2	5.2	5.9		5.5	5.7 ± 0.1
Si	7.1 ± 0.1	7.2 ± 0.2	7.3 ± 0.2	7.3 ± 0.2	7.5 ± 0.1	6.7 ± 0.1	7.1 ± 0.2	7.2	6.1 ± 0.1	7.0 ± 0.2
P					6.5 ± 0.3			5.8 ± 0.2	4.9	
S	7.0 ± 0.2	7.0 ± 0.3	7.3 ± 0.1	6.7 ± 0.1	7.4 ± 0.2	6.5	6.8 ± 0.1	7.1 ± 0.3	5.8 ± 0.1	6.4 ± 0.1
Ca	5.1 ± 0.3	5.4 ± 0.4	5.3 ± 0.2	5.0 ± 0.3	5.3 ± 0.2	5.0 ± 0.3	5.3 ± 0.3		5.0 ± 0.3	5.1 ± 0.2
Sc		3.2			2.8 ± 0.1			3.5	1.9	2.9 ± 0.1
Ti			4.1 ± 0.3		3.5 ± 0.3	3.7		4.0	3.1	4.1 ± 0.2
Fe	6.3 ± 0.2	6.3 ± 0.3	6.7 ± 0.2	5.8 ± 0.2	5.6 ± 0.2	6.1 ± 0.3	6.4 ± 0.3	6.3 ± 0.2	5.5 ± 0.2	6.0 ± 0.1
Ni	5.8 ± 0.2	5.6 ± 0.3	5.9 ± 0.2	5.2 ± 0.1	5.8 ± 0.1	5.4	5.7 ± 0.3			5.9 ± 0.1
Zn	4.1	4.4	4.5	3.9	4.1	3.6	4.3		3.6	4.4 ± 0.3
Y	2.0	2.4 ± 0.2	1.9 ± 0.2	2.8 ± 0.1	1.3 ± 0.5	1.3 ± 0.1	1.9 ± 0.3		2.1	2.2 ± 0.2
Zr	2.3 ± 0.2		1.8 ± 0.2	2.6 ± 0.1						2.1 ± 0.2
Ba	1.4 ± 0.3	1.2 ± 0.2	1.4 ± 0.2	1.4 ± 0.3	0.9 ± 0.2	0.3 ± 0.1	1.5 ± 0.1		0.6 ± 0.3	1.3 ± 0.1
La		0.8	1.0 ± 0.4		0.5					0.4 ± 0.1

[a] Spectroscopic C I abundance which differs from assumed input abundance of 9.5 corresponding to C/He=1%, except for V854 Cen for which an input abundance of 10.4 (C/He=10%) was assumed

to the available lines being quite strong with low excitation energies. These comparisons suggest that the X/Fe ratios for most elements are quite insensitive to the adopted models. Of course severe line-blanketing, and more so than for H-rich stars, is a reality in R CrB stars and must therefore be accounted for.

5.1.3. Effects of model atmosphere abundances

The input abundances for our model atmosphere grid were taken from Lambert & Rao (1994) who used the non-blanketed models for their abundance analysis. In short, adopted and derived abundances are inconsistent. We have reanalysed R CrB with new models computed with the lower derived abundances, though

Table 4. Errors due to uncertainties in the stellar parameters of RY Sgr, defined by $\Delta(\log \epsilon_i) = \log \epsilon_i$(perturbed) - $\log \epsilon_i$(adopted). The adopted parameters are $T_{\rm eff} = 7250\,{\rm K}$, $\log g = 0.75\,[\rm cgs]$ and $\xi_{\rm turb} = 6.0\,{\rm km\,s^{-1}}$

Species	$\Delta T_{\rm eff} = -250$ [K]	$\Delta \log g = -0.5$ [cgs]	$\Delta \xi_{\rm turb} = -1.0$ [km s^{-1}]
H I	$+0.17$	-0.10	$+0.08$
Li I[a]	-0.23	$+0.16$	$+0.00$
C I	-0.05	$+0.06$	$+0.07$
N I	$+0.14$	-0.12	$+0.07$
O I	$+0.09$	-0.13	$+0.13$
Na I	-0.16	$+0.15$	$+0.07$
Al I	-0.16	$+0.14$	$+0.02$
Si I/II	$-0.15/+0.09$	$+0.14/-0.19$	$+0.07/+0.19$
S I/II	$-0.11/+0.28$	$+0.11/-0.29$	$+0.14/+0.10$
Ca I	-0.27	$+0.26$	$+0.04$
Ti II	-0.06	-0.11	$+0.10$
Fe I/II	$-0.21/+0.01$	$+0.16/-0.14$	$+0.06/+0.18$
Ni I	-0.22	$+0.15$	$+0.01$
Zn I	-0.18	$+0.15$	$+0.07$
Y II	-0.11	-0.05	$+0.04$
Zr II	-0.09	-0.09	$+0.01$
Ba II	-0.29	$+0.12$	$+0.28$
La II	-0.22	$+0.03$	$+0.02$

[a] Adopting $W_{6707}({\rm Li\,i}) = 10\,{\rm m\AA}$, which is the observed upper limit.

still assuming C/He=1%, which leads to less line-blanketing. The effects on the deepest layers are, however, minor and the carbon problem is not appreciably alleviated, since many of the lines contributing the backwarming remain highly saturated. The abundances derived from the new models are within 0.2 dex of the revised input abundances, but a slight revision of the stellar parameters seems necessary. After restoration of the ionization equilibria by lowering $\log g$ by 0.5 dex, the absolute abundances differ from those provided by the standard grid by $\lesssim 0.05$ dex except for H and Y where the differences are 0.1 and 0.2 dex, respectively. We conclude that the inconsistency between adopted and derived abundances does not affect our results significantly.

As a test, one of the stars (UX Ant) was also reanalysed with all model abundances being consistent with the derived abundances, i.e. the models had a sufficiently low C/He ratio (0.04%) such that the carbon problem disappeared. Except for the C II lines, the various $T_{\rm eff}$-$\log g$ indicators suggest the same stellar parameters, though with a slightly larger scatter. All derived abundances are naturally smaller by more than 1 dex, but the relative abundances remain essentially the same: in all cases X/Fe changes by $\lesssim 0.2$ dex. For the minority stars, a consistent C abundance would lead to very low metallicities, about 2.5 dex below solar.

5.1.4. Effects of uncertainties in stellar parameters

The uncertainties in the adopted stellar parameters translate into errors in the derived abundances. The parameters are estimated to be accurate to within typically $\Delta T_{\rm eff} = \pm 250\,{\rm K}$,

$\Delta \log g = \pm 0.5\,[\rm cgs]$ and $\Delta \xi_{\rm turb} = \pm 1\,{\rm km\,s^{-1}}$. These uncertainties correspond to typical abundance errors of 0.2 dex for most elements, as shown in Table 4. For Ca and Ba the errors may reach 0.4 dex. Abundance ratios are generally much less subject to uncertainty, since most elements are similarly sensitive to the parameters. Notable exceptions are N/Fe and O/Fe, for which we estimate typical errors of 0.3–0.4 dex.

5.1.5. Effects of a perturbed temperature structure

As seen above, a possible resolution to the carbon problem is a very perturbed temperature structure compared with model predictions. The effect on the derived abundances of such an adjustment has been estimated for three stars spanning a range in $T_{\rm eff}$ with models such that the carbon problem is eliminated. It is noteworthy that use of such models does not change the ionization equilibria or $\xi_{\rm turb}$. Thus, we may assume that the adopted stellar parameters are not in need of substantial revision, though the heated models do impair the ability to obtain a comprehensive fit to the He I, C II, and C$_2$ features. In Table 5 the differences in absolute and relative abundances between the heated and standard models are given. Table 5 shows that the quite drastic changes in the temperature profile have rather limited effects on abundance ratios, generally less than ± 0.2 dex, though a few elements show somewhat larger differences of up to ± 0.4 dex for the hottest stars.

5.1.6. Effects of departures from LTE

Except for in the case of carbon, possible departures from LTE have not been investigated. One may fear, however, that such effects can be severe in these low-density atmospheres. Possible guidance can perhaps be provided by studies of H-rich supergiants with roughly the same $T(\tau)$ and $P_{\rm e}(\tau)$ structures in the line-forming region as R CrB stars. We find that a model with $T_{\rm eff} = 7000$, $\log g = 1.0$ and [Fe/H]=+0.5, roughly simulates an R CrB model with $T_{\rm eff} = 7000$, $\log g = 0.5$ and C/He=1%. The H-rich model, however, still has not a sufficiently steep $T(\tau)$ compared with the H-deficient model. The flux distributions of the two models are shown in Fig. 5. As expected, the H-rich model has more flux in the blue due to less line-blocking. Only just bluewards of the Balmer jump are the fluxes in the H-rich model somewhat smaller than the corresponding R CrB model. This suggests that overionization should be a less troublesome worry in R CrB models. Furthermore, the densities are higher in the H-deficient atmosphere on account of the lower continuous opacities, which should lead to more efficient thermalization.

Few statistical equilibrium calculations for F supergiants have been undertaken to date. Venn (1996) finds large departures from LTE for C and N ($\Delta \log \epsilon = \log \epsilon_{\rm nlte} - \log \epsilon_{\rm lte} \simeq -0.3$ dex). Considering the minor non-LTE effects for C found in R CrB stars (Asplund & Ryde 1996), this suggests that LTE is in general a better description in R CrB stars than in H-rich supergiants. For Na I, Boyarchuk et al. (1988) find only minor effects in F supergiants, and neither seems S to be significantly hampered by departures from LTE ($\simeq -0.2$ dex, Takeda & Takada-Hidai
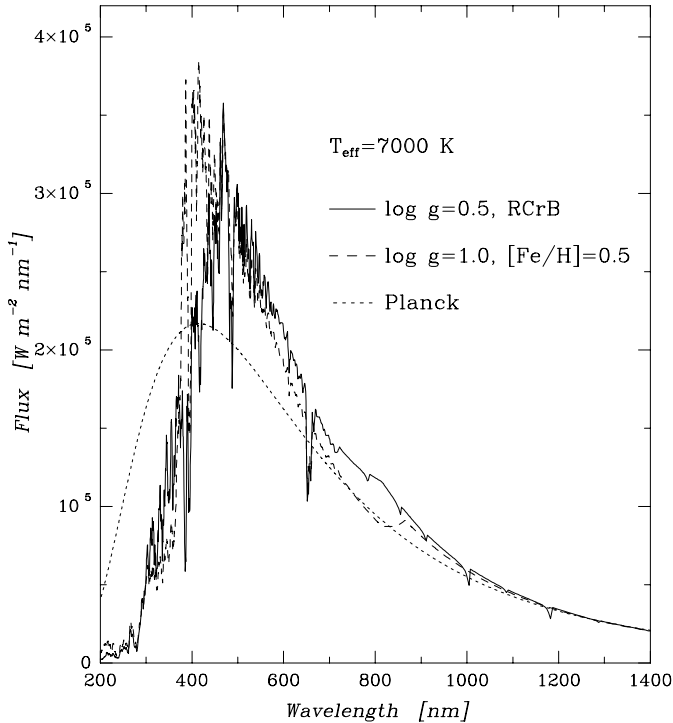
Fig. 5. Flux distributions for an R CrB model (C/He=1%) and a H- and metal-rich ([Fe/H]=+0.5) supergiant with roughly similar $T(\tau)$ and $P_e(\tau)$ structures. Both models have $T_{\mathrm{eff}} = 7000$ but the R CrB model has $\log g = 0.5$ [cgs] while the H-rich model has $\log g = 1.0$. Also shown is a Planck curve for the same temperature

Table 5. The effects on absolute and relative abundances of heating the line-forming region in the model atmospheres[a] to eliminate the carbon problem. The listed logarithmic abundances and abundance ratios are relative to derived values using the standard models

	GU Sgr ($T_{\mathrm{eff}} = 6250$)		UX Ant ($T_{\mathrm{eff}} = 7000$)		V3795 Sgr ($T_{\mathrm{eff}} = 8000$)	
	ΔX	ΔX/Fe	ΔX	ΔX/Fe	ΔX	ΔX/Fe
H	-	-	0.88	0.31	0.13	-0.24
Li	0.47	-0.06	0.56	-0.01	-	-
C	0.68	0.15	0.66	0.09	0.69	0.32
N	0.26	-0.27	0.39	-0.18	0.27	-0.10
O	0.30	-0.23	0.54	-0.03	0.76	0.39
Na	0.60	0.07	0.43	-0.14	0.41	0.04
Al	0.61	0.08	-	-	0.36	0.00
Si	0.60	0.07	0.41	-0.18	0.58	0.21
S	0.73	0.20	0.55	-0.02	0.60	0.23
Ca	0.58	0.05	0.71	0.14	0.75	0.38
Fe	0.53	-	0.57	-	0.37	-
Ni	0.54	0.01	0.44	-0.13	0.48	0.11
Y	0.42	-0.11	0.32	-0.25	0.52	0.15
Ba	0.34	-0.19	0.48	-0.09	0.56	0.19

[a] Heated models (see Eqs. (6) and (7)) are defined by $b_1 = -2.5$, $b_2 = -0.5$ and the parameter a where $a = 900, 1000, 1500\,\mathrm{K}$ for GU Sgr, UX Ant and V3795 Sgr, respectively. The stellar parameters T_{eff}, $\log g$ and ξ_{turb} are as in Table 2.
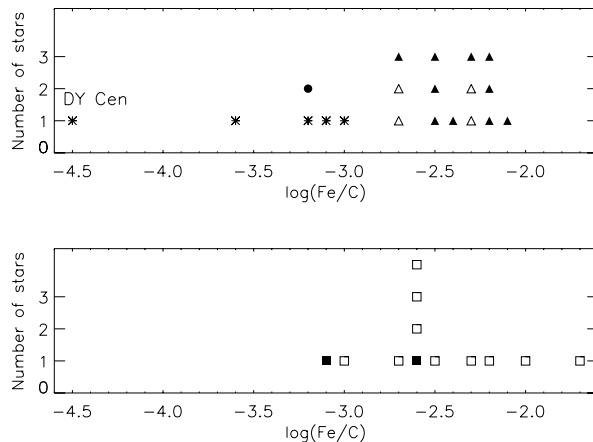

Fig. 6. Comparison of the derived spectroscopic Fe/C ratios for R CrB stars (upper panel) and EHe stars (lower panel). Symbols are as in Fig. 3, with the addition of DY Cen (classified as a minority star) and EHe stars from the literature (□)

1995). Gratton et al. (1999) conclude that Fe I suffers from a significant overionization in giants, which leads to erroneous abundances by $\simeq 0.3$–0.4 dex when using Fe I lines under the assumption of LTE. Gratton et al. also find that LTE analyses may overestimate O abundances significantly, but that Mg is reasonably well described.

It seems reasonable to conjecture that the N and O abundances may be systematically overestimated by up to $\simeq 0.5$ dex in our analysis, but that Na and Mg are less effected. An overionization of Fe I by 0.3 dex would lead to systematically too low $\log g$ by $\simeq 0.5$ dex, which, according to Table 4, would cause an increased Fe abundance by $\simeq 0.15$ dex; similar corrections would apply to other elements. The effects on relative abundance will thus be much smaller. One can speculate that also Ca I may be overionized for the same reason as Fe. Obviously, the derived abundances should be regarded as preliminary until detailed statistical equilibrium calculations have been performed, but it is clear that, e.g., the differences between the minority and majority R CrB stars are much too great to be blamed on non-LTE effects, in particular since the two groups have similar parameters and thus presumably similar departures from LTE.

5.1.7. Comparison with the EHe stars

External comparisons may also be used to check the analysis. Reasonable presumptions are that the R CrB stars form an evolutionary sequence with the EHe stars. EHe stars hot enough

to permit direct spectroscopic determination of the C/He ratio ($T_{\mathrm{eff}} \gtrsim 10000\,\mathrm{K}$) have a mean Fe/C$= -2.4 \pm 0.4$ (Jeffery 1996, 1998; Jeffery et al. 1998; Drilling et al. 1998), which corresponds to Z(Fe)$= 10^{-3.4 \pm 0.4}$; here two EHe stars with unusually low C/He ratios have been excluded. With the spectroscopic C abundance, the majority R CrB stars give a mean ratio Fe/C$= -2.4 \pm 0.2$. As shown in Fig. 6, the R CrB minority has distinctly lower metallicity (Fe/C). The mean Fe/C for the minority including V854 Cen (Asplund et al. 1998) and Sakurai's object (Asplund et al. 1997b, 1999) is 0.8 dex less than
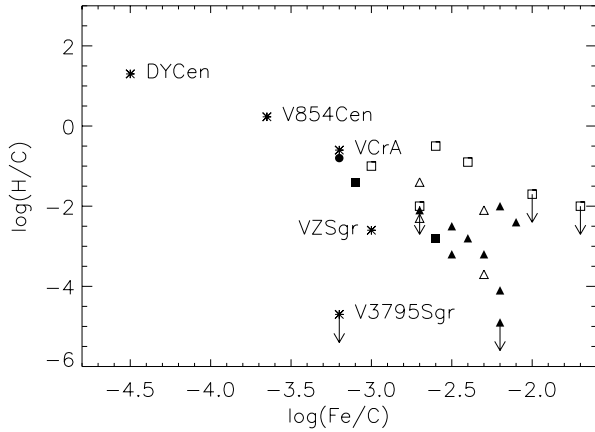
Fig. 7. The logarithmic H/C vs Fe/C ratios in hydrogen-deficient stars: The symbols correspond to Li-rich majority members ($\triangle$), other majority stars (black triangles), the minority R CrB stars (including V854 Cen and DY Cen) ($*$), our EHe stars (black squares), EHe stars ($\square$) from the literature, and Sakurai's object in October 1996 ($\bullet$) (Asplund et al. 1999). For the ratios, the spectroscopic C abundances have been used. Upper limits are denoted by arrows

for the majority. As is evident from Eq. (2), such differences do not necessarily reflect differences in the mass fraction Z(Fe) but may be due to a higher C/He ratio.

The comparison shows that the spectroscopic Fe/C is similar for R CrB stars and EHe stars as regards mean and dispersion, as seen in Fig. 6. The similarity suggests that spectroscopic ratios give results little affected by systematic errors. Note that the derivation of elemental abundances for R CrB and EHe stars generally employ different lines and model atmospheres and, hence, systematic errors are likely to be different for the two samples.

5.1.8. Summary of abundance uncertainties

In spite of the uncertainties introduced by the unresolved carbon problem, the tests presented above suggest that it does not render conclusions regarding abundances impossible, in particular not if abundance ratios are considered. Ratios such as X/Fe are not very sensitive to details of the model atmospheres (blanketed vs non-blanketed, postulated heating etc). Furthermore, the R CrB stars and EHe stars fortunately show extreme abundance ratios which will not disappear with any reasonable alternative model atmosphere, and thus important clues to the origins of the stars can still be deduced. Disregarding possible departures from LTE, the systematic errors in X/Fe are expected to be typically $\lesssim 0.2$–0.3, though some elements are probably more prone to errors. The small observed dispersions in derived abundances for most of the elements in our sample also suggest that the errors are not very severe.

5.2. *Abundances relative to iron*

In Table 6 the mean abundances relative Fe are summarized for elements measured in the majority R CrB stars. H and Li are not

included due to their large abundance range across the sample, nor are a few other elements which have been determined in only a few stars. Table 6 also includes abundance ratios for the minority R CrB stars (with values for V854 Cen taken from Asplund et al. 1998), our two cool EHe stars, EHe stars from the literature (excluding two unusual EHe stars), and Sakurai's object (Asplund et al. 1999). A remarkable result is that, with the exception of O, Y and Ba, the dispersions (0.1–0.3 dex) suggest no significant intrinsic scatter in [X/Fe] for the R CrB majority. The dispersions are nominally larger (0.4–0.6 dex) for the EHe stars for the few elements common to both samples. From the published analyses of EHe stars it is difficult to assess whether the dispersions reflect an intrinsic spread in [X/Fe] or are merely a consequence of measurement errors. Unfortunately, the Fe abundance is often poorly determined in EHe stars due to lack of lines and atomic data, which might affect the comparison with the R CrB stars. We have, however, still preferred to discuss X/Fe ratios rather than e.g. the spectroscopic X/C ratios, since according to the tests in Sect. 5.1, X/Fe is less affected by the unresolved carbon problem and uncertainties in the adopted stellar parameters.

5.2.1. Hydrogen

By definition, our sample is H-deficient, but there is a large range in observed H abundances: from 8.0 (V CrA) to < 4.1 (XX Cam and V3795 Sgr). There are also R CrB stars with only a relatively minor H-deficiency: V854 Cen with 9.9 (adopting C/He=10%, Asplund et al. 1998) and DY Cen with 10.8 (Jeffery & Heber 1993). Two of the minority stars have high H abundances (V854 Cen and V CrA), though this group also contains the most H-deficient star (V3795 Sgr). The large spread in H abundance indicates that the amount of pristine material in the stellar atmospheres varies greatly between the objects; the deficiency ranges from only a factor of 20 to $> 10^8$.

There is an apparent anti-correlation between the H and Fe abundances according to Fig. 7, as first pointed out by Heber (1986); the only exception to the trend is V3795 Sgr. Also Sakurai's object follows the same pattern (Asplund et al. 1999). Since most metals are roughly proportional to Fe, H is also anti-correlated with many other elements. The H abundance is clearly very sensitive to the metallicity: increasing Fe/C by a factor of 100 leads to a decrease in H/C by about 4 orders of magnitudes. The reason for the H/C vs Fe/C trend is not immediately obvious. Since the core mass of post-AGB stars decreases with higher metallicity for given initial stellar mass (Han et al. 1994), and the envelope mass increases strongly with decreasing core mass (Paczyński 1971), one would naïvely expect that the H-rich envelope should be more easily burnt and diluted with core material for a lower metallicity, which is opposite to the observed relationship.

5.2.2. Lithium

Four of the R CrB stars (UW Cen, R CrB, RZ Nor and SU Tau) are Li-rich, which places important constraints on the proposed

Table 6. The logarithmic abundance ratios [X/Fe] for the R CrB stars, EHe stars and the final flash candidate Sakurai's object. For the R CrB majority (14 stars) and the EHe stars taken from the literature (10 stars, excluding V652 Her, HD 144941, and the hot R CrB stars DY Cen, MV Sgr and V348 Sgr) the dispersion is also given in parentheses

Element ratio [X/Fe][a]	R CrB stars					EHe stars			Sakurai's object (Oct '96)[d]
	majority	minority				LS IV $-14°109$	BD $1°4381$	others[c]	
		V3795 Sgr	VZ Sgr	V CrA	V854 Cen[b]				
N	1.7 (0.3)	2.0	1.4	2.8	1.4	1.9	1.3	0.9 (0.3)	1.9
O	0.4 (0.6)	0.6	1.6	2.0	1.6		1.7	0.3 (0.7)	1.5
Na	0.8 (0.1)	1.5	1.2	1.7	1.6	1.3	1.1		1.4
Al	0.5 (0.3)	1.0	0.6	0.9	0.7		1.0	0.2 (0.4)	0.7
Si	0.6 (0.2)	1.9	1.5	2.2	1.0	0.9	0.6	0.4 (0.5)	0.9
S	0.6 (0.3)	2.0	1.1	2.3	0.6	1.0	0.5	0.3 (0.5)	0.5
Ca	0.0 (0.2)	0.8	0.3	0.8	0.2		0.6	0.5 (0.1)	0.0
Ni	0.6 (0.2)	1.4	0.6	1.4	1.1			0.1 (0.3)	0.8
Y	0.8 (0.4)	1.0	2.3	0.5	1.5		1.9		2.9
Ba	0.4 (0.4)	0.7	1.0	0.7	0.7		0.5		0.7

[a] Solar abundances taken from Grevesse & Sauval (1998).
[b] From Asplund et al. (1998).
[c] From Jeffery (1996), Jeffery (1998), Jeffery et al. (1998) and Drilling et al. (1998)
[d] From Asplund et al. (1999).
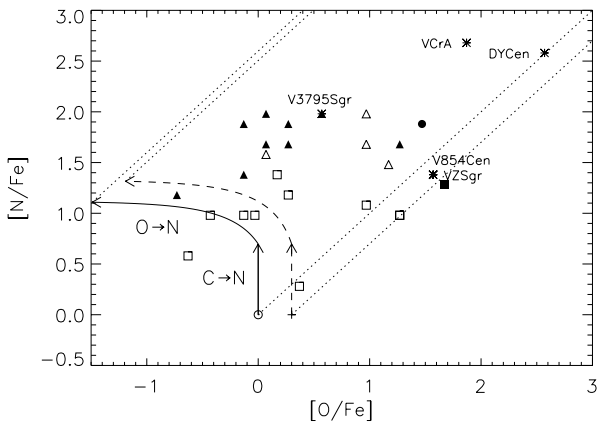
Fig. 8. [N/Fe] vs [O/Fe] for R CrB stars and EHe stars. The symbols have the same meaning as in Fig. 7 with additions for the Sun ($\odot$) and typical halo dwarf abundances for [Fe/H] $\simeq -1.0$ (+). The C→N trajectory correspond to the N enrichment by CN-cycling for an initial solar (solid) and a metal-poor (dashed) composition. The O→N trajectory is the same when also the initial O is converted to N through ON-cycling. If Fe but neither N nor O is being depleted, the star will move along trajectories with the same 1-to-1 slope as the dotted curves

models for the formation of the stars. That all four stars belong to the majority group may be significant but could also be an effect of small number statistics. The Li abundances for the four range from 2.6 to 3.5 with a mean of 3.1, while the other RCrB stars have upper limits from 2.5 to 1.0. Pollard et al. (1994) also claim the presence of Li in two of the LMC R CrB stars, which both seem to belong to the majority. Vanture et al. (1999) tentatively identify the Li I 6708 Å line in the strongly s-element rich R CrB star U Aqr but its crowded spectrum prevents a secure membership classification.

Our Li/Fe ratio for R CrB is about 0.3 dex smaller than found by Hunger et al. (1982) using non-blanketed models. There is no obvious trait of the Li-rich group besides the high Li abundance and possibly that the H abundance is relatively high for these majority R CrB stars, with the exception of RZ Nor.

The similarity with the cosmic Li abundance for the group is most probably fortuitous, since H-burning destroys fossil Li. The high Li abundances can thus neither stem from a previous AGB-phase but must have been synthesized simultaneously with or subsequently to the events which turned the stars into H-deficient R CrB stars. In this context it is interesting to note that Sakurai's object, which is thought to have experienced a final He-shell flash recently, shows a rapidly increasing Li abundance and H-deficiency (Asplund et al. 1997b, 1999).

5.2.3. Nitrogen and oxygen

N and O are principal clues to the origins of the R CrB stars. N enrichment is a certain result of H-burning by the CNO-cycles but N is destroyed by α-captures prior to ignition of He. Then, the N abundance indicates the relative mix of products from H- and He-burning. O is a product of He-burning with the relative yields of C and O depending on the burning temperature.

The R CrB majority stars share a common N/Fe ratio but probably exhibit an intrinsic spread in their O/Fe ratios as seen in Fig. 8. DY Cen and the minority R CrB V CrA are clearly outstanding in both [N/Fe] and [O/Fe]. The [N/Fe] of the EHe stars (excluding DY Cen) appears to be systematically lower by about 0.8 dex than for the majority of the R CrB stars. The two samples appear to have quite similar distributions for [O/Fe]. The dispersion in [N/Fe] of the majority sample of R CrB stars is 0.2 dex and consistent with the measurement errors. [O/Fe] shows a larger dispersion (0.6 dex) to which an appreciable contributor must be a star-to-star spread in O/Fe ratios. A similar

difference in the dispersion of [N/Fe] and [O/Fe] is found for the EHe stars (0.3 and 0.7 dex).

N enrichment is anticipated from contamination of initial material with products from H-burning. If the initial composition is solar and the CN-cycle operates efficiently, [N/Fe] is raised to 0.7, which still is less than for all observed R CrB stars: the mean [N/Fe] for the R CrB majority is 1.6. If the ON-cycles convert O to N, [N/Fe] increases to 1.1 as O/Fe decreases, as shown by the trajectory O→N in Fig. 8. This trajectory grazes the left edge to the distribution of the points in the figure. For a composition representative of metal-poor stars, [O/Fe] ≃ 0.3 but [C/Fe] ≃ [N/Fe] ≃ 0.0 (Wheeler et al. 1989), which displaces the trajectories to higher [N/Fe] and [O/Fe] values. Very few of the observed abundance ratios fall between these trajectories. If the Fe abundance is representative of the original composition, the high N abundance implies further CNO-cycling from He-burning products, which is required to account for the high C/He. Since V CrA and DY Cen also have apparently lower metallicities than others, it is possible that the high [N/Fe] and [O/Fe] may result from a depletion of Fe; a factor of 10 depletion of Fe would convert a R CrB majority star into one of these minority members.

5.2.4. Sodium and aluminium

Relative to Fe, Na and Al appear overabundant: [Na/Fe] ≃ 0.8 and [Al/Fe] ≃ 0.5. For the EHe stars, Al is similarly overabundant but the status of Na is uncertain owing to a lack of data. A remarkable result is that there appears to be no intrinsic scatter in [Na/Fe] (Fig. 9) and [Al/Fe] (Asplund et al. 1998) for the R CrB majority. The minority R CrB stars extend from the cluster defined by the majority to higher [Na/Fe] and [Al/Fe], though the separation in [Al/Fe] is less distinct. Qualitatively, the Na and Al enrichments are as expected from material severely exposed to H-burning: Na is enriched by proton capture on ^{22}Ne and Al by proton capture on ^{26}Mg.

5.2.5. Silicon, sulphur, calcium and nickel

Fig. 10 shows that the combined sample of R CrB stars and EHe stars defines the linear relation [Si/Fe] ≃ [S/Fe]. For the R CrB majority, [Si/Fe] ≃ [S/Fe] ≃ 0.6. Minority R CrB stars are clearly offset in both [Si/Fe] and [S/Fe] from the majority with DY Cen remarkably outstanding. The EHe stars have typically slightly smaller [Si/Fe] and [S/Fe] ratios than the R CrB majority.

The high [Si/Fe] and [S/Fe] ratios of the minority R CrB stars, DY Cen and possibly a couple of the EHe stars cannot be due to either initial composition of the H-rich progenitor or systematic errors. Either nuclear processing has enriched Si and S (relative to Fe) or chemical processes (e.g. a dust-gas separation) have altered these ratios significantly. In the extreme cases of DY Cen and V CrA, Fe must have been depleted by a factor of almost 100 if neither Si nor S have been depleted.

According to Fig. 11 the dispersion in Ca/Fe for the R CrB majority is small and again the offset of the minority R CrB
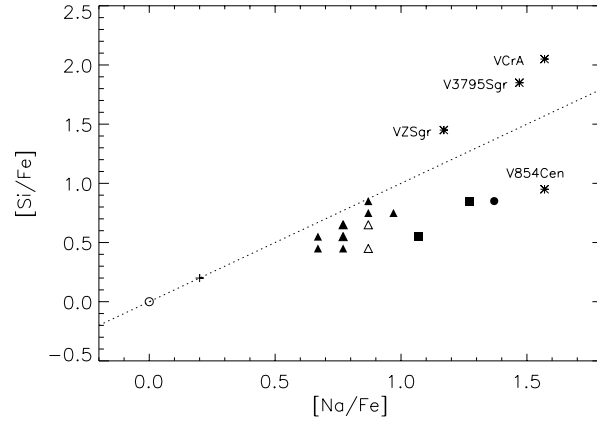

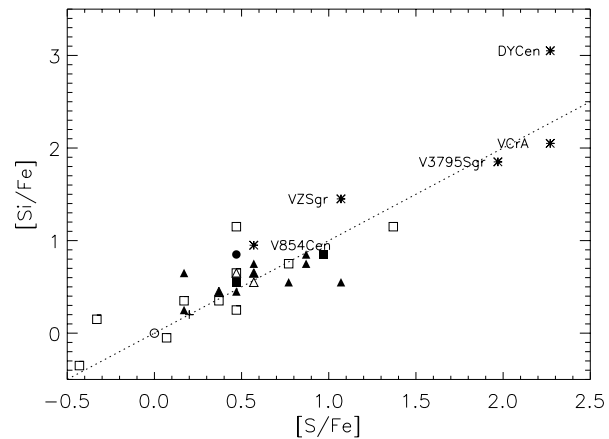**Fig. 9.** [Si/Fe] vs [Na/Fe] for R CrB stars and EHe stars. The symbols have the same meaning as in Fig. 8

Fig. 10. [Si/Fe] vs [S/Fe] for R CrB stars and EHe stars. The symbols have the same meaning as in Fig. 8

stars is clear. There is a hint that Ca is systematically enriched in EHe stars or depleted in R CrB stars but additional observations are desirable; the Ca abundances are highly dependent on strong lines in both samples. Minority R CrB stars have higher [Ca/Fe] ratios than the majority stars. Unfortunately, DY Cen's Ca abundance is unknown.

Ni in the R CrB majority is overabundant ([Ni/Fe] ≃ 0.6) and with a small dispersion, as shown in Fig. 12. The minority R CrB stars on average have a higher [Ni/Fe]. The two EHe stars for which Ni abundances have been determined have a mean at the solar ratio. Since the sensitivities of the Ni I and Fe I lines to atmospheric structure are quite similar, [Ni/Fe] cannot be reduced to the solar ratio by use of reasonable alternative models.

5.2.6. Yttrium and barium

The light s-elements are represented in our analysis by Y and to some extent Zr, while the heavy s-elements are present as Ba with confirming lines of La in some cases. Our results show that the heavy elements relative to Fe are overabundant in R CrB stars: [Y/Fe] ≃ 0.8 and [Ba/Fe] ≃ 0.4 for the majority, which

Fig. 11. [Si/Fe] vs [Ca/Fe] for R CrB stars and EHe stars. The symbols have the same meaning as in Fig. 8

Fig. 12. [Si/Fe] vs [Ni/Fe] for R CrB stars and EHe stars. The symbols have the same meaning as in Fig. 8
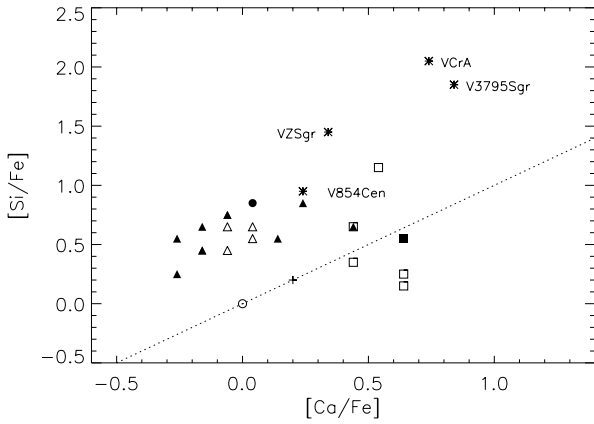

Fig. 13. The s-elements [Y/Fe] vs [Ba/Fe] in R CrB stars and EHe stars. The symbols have the same meaning as in Fig. 8

suggests the presence of material exposed to s-processing. There is no striking difference between the R CrB majority and minority. There is an intrinsic spread in the heavy element abundances but with a correlation between the Y and Ba abundances (Fig. 13). Abundances of heavy elements are unfortunately not available for the hot EHe stars. Both the Y and Ba abundances are anti-correlated with the H abundances, which presumably reflects the anti-correlation found between H and Fe, since Fe is the seed nuclei for s-processing.

Ba abundances in two R CrB stars have been studied together with their Li abundances by Hunger et al. (1982). Our Ba/Fe ratios are 0.5–1.0 dex smaller which presumably reflects our much superior spectra and model atmospheres. Further comparison is therefore difficult, though the overabundance of Ba is clear in both cases. Vanture et al. (1999) find extraordinary over-abundances of s-elements in U Aqr (e.g. [Y/Fe]=3.3 and [Ba/Fe]=2.1), which are off-scale in Fig. 13, even compared to Sakurai's object. However, these abundances are based only on very strong lines in a very crowded spectrum and the results can therefore be expected to be quite uncertain.

5.2.7. Summary of abundance trends

Given the carbon problem, we have to take all abundances derived for R CrB stars with balanced scepticism. However, various tests seem to indicate that credibility, on the 0.2 dex level, could be ascribed to abundance ratios. Furthermore, the significant differences between the abundance ratios of the R CrB stars and solar-type stars or halo dwarfs for many elements, as well as between the two different groups of R CrB stars, are unlikely to vanish with any alternative model atmospheres. Thus, many conclusions regarding the evolutionary history of the stars can still be drawn, in spite of the uncertainties introduced by the carbon problem.

Among the different abundance trends found the following are worth emphasizing:

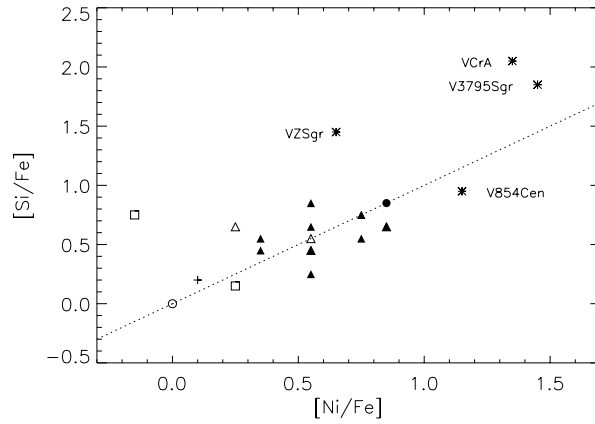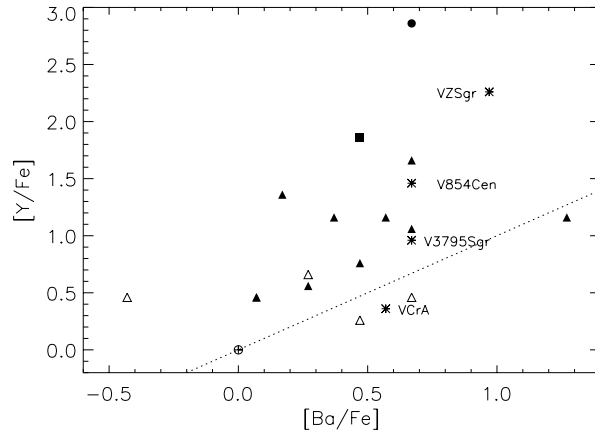1. The R CrB stars can be divided into a homogeneous majority group and a diverse minority, which is distinguished by a low metallicity and extreme abundance ratios, in particular as regards Si/Fe and S/Fe. The majority shows little star-to-star scatter except for H, Li, O, Y and Ba.
2. The H abundance is anti-correlated with the abundance of Fe for both the majority and the minority as well as for the EHe stars (Fig. 7).
3. The Li abundance is high for four R CrB stars, which all belong to the majority group.
4. There are considerable enrichments of N and sometimes also of O (Fig. 8).
5. Al/Fe, Na/Fe, Si/Fe and S/Fe exceed the solar values (Figs. 9 and 10).
6. Ca/Fe is about solar, though some minority stars have significantly higher ratios (Fig. 11).
7. Ni is enriched relative to Fe (Fig. 12).
8. The s-elements are enriched relative to Fe, the light s-elements more than the heavier elements (Fig. 13).
9. The minority stars tend to show extreme positions along the trends discussed above. Thus, they have in general high H, low Li, high N, O, Na, Al, Si, S, Ca, Ni and Zn abundances relative Fe (Figs. 7-12). This may possibly also be true for

Y and Ba (Fig. 13). The scatter for the minority is greater than for the majority.

10. Judging by chemical composition, Sakurai's object resembles the R CrB stars (Asplund et al. 1997b, 1999), but in different aspects both the majority and the minority, which is also true of the R CrB star V854 Cen (Asplund et al. 1998).

Although some of these tendencies may be considerably affected by systematic errors, e.g. departures from LTE, we judge them to be grossly real.

6. Abundance analysis – interpretation

6.1. The basic processes

Before interpreting the derived abundances in terms of the evolution for these H-deficient stars, one must first identify the various processes which may have been responsible for producing the exotic chemical compositions of the stars. Clearly, R CrB and EHe stars are in late stages of stellar evolution and many elemental abundances must have been affected by nucleosynthesis during the lifetime of the stars. Furthermore, given the observational evidence that similarly (H-rich) luminous stars have photospheres depleted in elements that easily condense into grains (cf. Lambert 1996), it is possible that also R CrB stars have suffered a similar fate. The possible systematic errors discussed in Sect. 5.1 must also be kept in mind in the following.

6.1.1. Comparison with halo stars

To be able to determine which nuclear and chemical processes have been at work in the stars, it is necessary to first estimate the initial abundances. As already mentioned, the spectroscopic Fe/C ratios together with the adopted C/He ratio suggest that the R CrB majority stars are only mildly metal-poor, $[Z(Fe)] \simeq -0.4$. For Ca, which is not expected to be altered in connection with H- and He-burning, the abundance relative Fe in galactic disk dwarfs increases slowly with decreasing metallicity (Edvardsson et al. 1993). For the R CrB majority $[Ca/Fe] \simeq 0.0$ is as expected for stars with $[Fe/H] \simeq -0.4$. The lack of dispersion for R CrB stars is then consistent with the similar lack in the dwarfs. For the minority stars an initial metal-poor composition cannot, however, be invoked to explain the high $[Ca/Fe]$.

With decreasing $[Fe/H]$ for disk and halo dwarfs, $[Si/Fe]$ and $[S/Fe]$ increase until $[Fe/H] \simeq -1.0$ after which they are constant at the level $[Si/Fe] \simeq [S/Fe] \simeq 0.4$ (Wheeler et al. 1989). At a given $[Fe/H]$, there is essentially no intrinsic dispersion in the Si/Fe ratios for disk stars (Edvardsson et al. 1993). The high Si/Fe and S/Fe ratios for the minority R CrB stars are therefore not consistent with the stars being initially metal-poor. The ratios for the majority stars may also be too high to be pristine. Neither can the high $[Ni/Fe]$ ratios for either group be attributed to an initial composition as $[Ni/Fe] \simeq 0.0$ for disk and halo dwarfs (Edvardsson et al. 1993).

The remaining elements show definite marks of having been influenced by nuclear and/or chemical processes. Besides the obvious H, C, N and O, both Na and Al seem to be enriched. Also, the abundances of heavy elements are not indicative of compositions of unevolved stars for which $[Y/Fe] \simeq [Ba/Fe] \simeq 0.0$ for disk and halo dwarfs down to $[Fe/H] \simeq -2$.

6.1.2. Dust-gas separation

The abundances in the interstellar medium (ISM) differ distinctly from typical stellar abundances for many elements. This has been attributed to a dust-gas separation: easily condensable elements are tied up in dust grains. Similar abundance anomalies which correlate with the ISM depletions have been observed in various post-AGB stars (cf. Lambert 1996). A probable mechanism is that dust particles are removed from the gas which subsequently is accreted back onto the star. Considering the post-AGB status of the R CrB and EHe stars and their peculiar abundance ratios it is conceivable that their atmospheres have also been affected by depletion.

It is clear that dust-gas separation, as it occurs in the ISM, cannot explain all of the observed abundance ratios in R CrB and EHe stars. The degree to which this is so is, however, dependent on whether the depletions observed in dense interstellar clouds or those observed in intercloud regions are regarded more characteristic (cf. Jenkins 1987). If depletions characteristic of dense clouds are assumed to have occurred in R CrB stars, depletion cannot explain most of the abundance peculiarities found. Although the high Na and S abundances could be consistent with such a process, since they are little depleted in the ISM, the proposal fails as regards Al and Ca: both elements are among the most severely depleted and more so than Fe, which would lead to a smaller Al/Fe and Ca/Fe. Furthermore, the observed high Si abundances, in particular the extreme Si/Fe ratios of the minority, are difficult to reconcile with such an explanation. With the observed ISM depletions in ζ Oph (Savage & Sembach 1996), the $[Si/Fe]$ and $[S/Fe]$ ratios in the R CrB stars would be raised to give the wrong slope to the observed relation in Fig. 10.

However, if the intercloud results (cf. Jenkins 1987) are regarded characteristic for the depletion of R CrB stars, abundances of most intermediate mass elements (Na, Al, Si, S, Ca, Ti, Fe, Zn) for the majority come out roughly right (within about a factor of 2). The only exceptions are Mg, for which the observed abundance is about 1 dex lower than expected, and Ni, which is observed to be about 1 dex more abundant than the depletion hypothesis would suggest. Mg is, however, only available for 4 stars in the form of strong lines, while Ni may well have been affected by s-processing, as will be discussed below.

Another possibility is that the depletions in a H-deficient and C-rich gas differ markedly from typical ISM depletions. We are not aware of any published theoretical predictions of the effects of dust-gas separation in such environments, and cannot draw any decisive conclusions in this respect. Naïvely the high Si/Fe ratios are problematic since C-rich gas is expected to condense into SiC. In C-rich environments, other likely condensates are graphite and amorphous carbon, TiC, Fe, AlN and CaS (Lodders & Fegley 1995), which again is not readily reconciled with the observed abundances in R CrB stars.

In conclusion, it is not inconceivable that dust depletion has played a role in modifying the pre-R CrB star composition into rather close agreement with the presently observed atmospheric composition for elements from Na to Fe for the majority.

6.1.3. Nucleosynthesis

Nucleosynthesis has clearly left its mark on the composition of the R CrB stars. The atmospheres seem to contain material exposed to H-burning, followed by episodes of partial He- and H-burning, as well as s-processing. The presence of Li in some stars furthermore requires Li-synthesis. Some of the other over-abundances, most notably of Si and S in the minority, may also call for additional nucleosynthesis.

Of particular interest are the relative abundances of C, N and O as they give information on the relative amount of H- and He-burning. Since the N abundances exceed what is achievable by complete conversion of the initial C+N+O through CNO-cycling even for the majority R CrB stars, it seems that the He-burning products required to account for the high C/He ratio also provided additional C and O for a second episode of CNO-cycling. Mass fractions of H- and He-burning products can be estimated from the observed C/N ratio. We can for the moment assume that N has been synthesized from ^{12}C produced in He-burning; ON-cycling from freshly produced ^{16}O is assumed not to contribute significantly to the observed N. The observed C/Fe and N/Fe ratios for the majority then indicate that the atmospheres consist to about 2/3 of gas exposed to He-burning and 1/3 of material which has further been exposed to hot protons.

Additional support for a second phase of CNO-cycling comes from the high observed [Ne/Fe] ratios for the two stars in our sample where it has been determined. A similar Ne enhancement is also present in EHe stars. For V3795 Sgr and Y Mus, the high [Ne/Fe] cannot be explained by a complete conversion through α-captures on N from the initial C+N+O. Thus, we conclude that a second phase of CNO-cycling has taken place from which the generated ^{14}N has subsequently been exposed to α-particles and thereby produced ^{22}Ne. Further CNO-cycling would not be demanded if Ne was produced not by α-captures on ^{14}N seeds but through ^{16}O$(\alpha, \gamma)^{20}$Ne. The low Mg abundances argue against this possibility, since ^{20}Ne should experience additional α-captures and produce ^{24}Mg (e.g. Clayton 1968).

The overabundances of Na and Al may have been produced through proton captures, either on the AGB or, at least in the final-flash scenario, in connection with the ingestion of the H-rich envelope (Sect. 6.2). Unless the Si/Fe and S/Fe ratios have been affected by dust-gas separation, the high ratios for the majority seem to call for additional nucleosynthesis; this is even more the case for the minority R CrB stars with their extreme abundance ratios. An obvious choice for the responsible nuclear reactions is not readily available.

A signature of the R CrB stars is the enhancements of the s-process elements. The s-processing can be characterized by the neutron exposure τ_0 defined by

$$\tau_0 = \int_0^{t_{\exp}} N_{\mathrm{n}}(t) v_{\mathrm{T}} dt, \tag{8}$$

where N_{n} is the neutron density, v_{T} is the thermal velocity of the neutrons, and $t_{\exp}$ is the duration of exposure to neutrons. The heavy element abundances relative to Fe for the majority are consistent with a mild neutron exposure $\tau_0 \simeq 0.1 \, \mathrm{mb}^{-1}$ for a single exposure, while a value of $\tau_0 \simeq 0.05 \, \mathrm{mb}^{-1}$ seems more appropriate for an exponentially weighted exposure. According to Malaney (1987a) the expected abundance ratios for a single exposure of $\tau_0 \simeq 0.1 \, \mathrm{mb}^{-1}$ are log (X/Fe)=-0.7, -1.7, -4.7, -4.6 and -4.6, for X=Ni, Zn, Y, Zr and Ba, respectively; similar results are expected for an exponential exposure (Malaney 1987b). The corresponding observed ratios are -0.7, -2.1, -4.4, -4.6 and -4.9. Both types of exposures can also explain the otherwise problematically high Ni abundance, which suggests that the R CrB atmospheres consist mainly of material exposed to neutrons. Similar or possibly slightly larger neutron exposures seem appropriate for the minority stars, though in general the Ni/Fe ratios are more difficult to explain with exponential exposures in these stars. The high Sc abundance can also be explained by s-processing from Ca, as previously proposed for Sakurai's object (Asplund et al. 1997b, 1999) and FG Sge (Acker et al. 1982; Gonzalez et al. 1998). The dispersion in Y and Ba abundances indicates that the amount of s-processing varies significantly. The smaller dispersion in the Ni/Fe ratios compared with the Y/Fe and Ba/Fe ratios is consistent with expectations from s-processing with slightly different τ_0 (Malaney 1987a, 1987b).

For the s-processing, ^{13}C$(\alpha,$n$)^{16}$O is a probable neutron source. If the proton supply is large, CN-cycling will convert most of ^{12}C to ^{14}N, but if the protons are exhausted before the completion of the cycle, a large amount of ^{13}C may result with still a high C abundance (Renzini 1990). Upon exposure to He-rich gas at high temperatures ^{13}C$(\alpha,$n$)^{16}$O will be ignited, which will thereby liberate free neutrons to be used for s-processing. Despite the presence of neutron poisons such as ^{14}N, it is not inconceivable that the available neutrons are sufficient. The consumption of ^{13}C as a neutron source might prevent the isotope from being observed; a conservative lower limit to the ^{12}C/^{13}C ratio in R CrB is $\gtrsim 40$ (Cottrell & Lambert 1982). An alternative neutron source is ^{22}Ne$(\alpha,$n$)^{25}$Mg if the temperatures are higher. At least for Sakurai's object, the required neutron exposure ($\simeq 10$ neutrons per Fe seed nuclei) and the low observed Mg/Fe ratio ($\simeq 1$) are not consistent with ^{22}Ne being the neutron source.

The existence of a Li-rich subgroup of the majority R CrB stars places constraints on the proposed models for the formation of the stars. Most likely the stars have experienced Li-production through the Cameron-Fowler (1971) ^{7}Be transport mechanism. The lack of a detectable Li abundance in most of the R CrB stars could either be due to inefficient Li-production or that Li has once again be destroyed by exposure to high temperatures. As H-burning necessarily destroys Li, the observed Li must have been synthesized during or after the events which turned the stars into H-deficient stars.

6.2. Evolutionary scenarios

Two of the proposed explanations for the origin of the R CrB and EHe stars seem to be the most promising: the final-flash (here: FF, Renzini 1979) and the double degenerate (here: DD, Webbink 1984) conjectures. In the first scenario, a post-AGB star will experience a final He-shell flash after H-burning has been extinguished, which causes the H-rich envelope to be ingested and burnt. The liberated nuclear energy will expand the stellar envelope back to supergiant dimensions. The alternative scenario involves binary evolution: the immediate progenitors to the R CrB stars are assumed to be a pair of white dwarfs, which has been formed through mass transfer and common envelope episodes. If the pair is sufficiently close, emission of gravitational radiation will cause them to merge, which leads to ignition of He-burning and consequent inflation of the envelope. The pros and cons of the two scenarios have previously been discussed in detail by Renzini (1990), Schönberner (1996) and Iben et al. (1996), but the scenarios have not yet been confronted with the observed abundances of a large sample of stars. It is tempting to suppose that it is not a coincidence that observations suggest two groups as theory provides two scenarios.

At least one H-deficient giant, Sakurai's object (Asplund et al. 1999), has probably experienced a final flash. FG Sge, which is likely also a FF object, may be H-deficient (Gonzalez et al. 1998) and thus a new R CrB star. Other evidences for FF objects comes from the H-deficient PNe Abell 30, 58 (V605 Aql/Nova Aql 1919) and 78. The FF scenario also accounts for the presence of nebulosities around some R CrB stars (R CrB and UW Cen). According to Schönberner (1996), however, the life-times of the R CrB stars predicted by the FF scenario are too short. H-deficient giants formed through a merger are predicted to have longer life-times since their He-burning is stable rather than occurring as a flash. The DD scenario also naturally explains the fact that no R CrB or EHe star has been identified to be part of a binary system (but note the recent speculation that R CrB may be a binary system, Rao et al. 1999), while the observed nebulosities may possibly have formed during the merger process. The question is now whether decisive clues concerning the origin of the R CrB stars are provided by the observed abundances.

Unfortunately, the lack of detailed predictions of abundances in the different scenarios makes comparisons with observed abundance ratios not fully conclusive. Only two FF models have been discussed in the literature (Iben & MacDonald 1995; Herwig et al. 1999) but with incomplete nucleosynthesis, e.g. neither Li-production nor s-processing was investigated. For the DD scenario, the resulting chemical composition is quantitatively unknown, and especially so if nucleosynthesis occurs during or after the merger process.

Here, we shall first discuss observed abundances within the DD scenario. Accretion of a He white dwarf onto a C-O white dwarf directly explains the high He and N abundances in R CrB stars, as well as possibly the enrichment of Na and Al, which may have resided on the He white dwarf. A thin H-layer may have been present on the He white dwarf, but whether H can

Table 7. Summary of the pros and cons of the double degenerate (DD) and final flash (FF) scenarios in order to account for the observed properties of the majority and minority R CrB stars. When only one statement is given it applies to both groups, otherwise it applies to majority/minority, respectively

Property	DD	FF
H present	no?	yes
H vs Fe anti-correlation	?	?
Li present sometimes in majority	no/yes	yes
C/He	yes	no?/yes?
No ^{13}C	yes	no?
High N, O	yes	yes
High Na, Al	yes?	yes
High Si, S	?	?
s-process elements	yes?	yes
Abundance uniformity/non-uniformity for majority/minority	no?/yes	yes/no?
Similarity to Sakurai's object	no	yes
Nebulosities occasionally present	yes?	yes
Evolutionary time-scales	yes	no?
Lack of binarity	yes	no?

survive the merger is questionable. The high C and O abundances require mixing of material from the C-O white dwarf to the atmosphere of the resulting giant. Similar mixing is usually thought to occur on a O-Ne-Mg white dwarf in order to account for the composition of ejecta from a neon nova. Production of Li is unlikely. The scenario naturally explains the unobserved ^{13}C, since the isotopic abundance is very low following He-burning. The nuclear processes that will occur in connection with the merging are difficult to predict. One may speculate that the rp-process might synthesize the intermediate mass elements Na-S, as proposed in connection with novae on O-Ne-Mg white dwarfs (Politano et al. 1995). According to Politano et al. (1995), Mg and Ca should also be produced in significant amounts, which disagrees with the solar Mg/Fe and Ca/Fe ratios for the majority; the minority stars seem to have higher ratios however. In the merger of the He white dwarf with the C-O white dwarf, repeated α-captures may also occur, which might produce significant amounts of ^{28}Si and ^{32}S. It requires, however, a burning temperature of $\simeq 10^9$ K (Hashimoto et al. 1983). Such temperatures are higher than achieved in the simplified modelling of white dwarf mergers by Iben (1990) by at least a factor of two. The alternative that the abundances of the intermediate nuclei are determined by gas-dust separation cannot be excluded, but for the DD scenario this is then expected to occur after the merger, since the merger can be assumed to lead to such violent mixing processes that distorted abundance ratios confined to the surface layers are probably considerably reduced. It is probably more difficult to account for the s-process elements within the DD scenario, unless they are inherited from previous AGB phases.

A final He-shell flash naturally explains the high C and O abundances as products of He-burning. The high N abundances seem to require that additional N has been synthesized from

He-burning products, possibly through CN-cycling during the final flash. Proton captures can also account for the high Na and Al abundances while unburnt H may still be present in the atmospheres. As shown by Sakurai's object, Li production may occur. A potential fatal failure for the FF scenario is the high observed ^{12}C/^{13}C ratio in R CrB stars, since production of N through CN-cycling should also have resulted in large quantities of ^{13}C. According to Renzini (1990), the scenario might be saved if, after H-burning has ceased, ^{13}C is brought to higher temperatures due to the convective shell from He-burning. There it may react with α-particles and liberate free neutrons to be used for the necessary s-processing. ^{14}N may survive in spite of the destruction of ^{13}C, since the former only undergoes α-captures at higher temperatures. The difficulty in the FF scenario to account for the abundances of the intermediate elements may be solved by invoking gas-dust separation. As discussed above, the high Si/Fe is, however, not readily incorporated into such a scheme.

Another objection to the FF scenario voiced by Schönberner (1996) is the expected C/He ratio ($\simeq 5\% - 10\%$ by number, Iben & MacDonald 1995). Though C/He is poorly known for R CrB stars, a ratio larger than $\simeq 3\%$ is ruled out for the majority, unless the metallicity of the R CrB stars is assumed to exceed the solar value. Transformation of the superfluous C to O through α-capture starting with C/He$\simeq 10\%$ is not an option as it would be in conflict with the observed C/O ratio. Furthermore, recent modelling which includes convective overshoot in a parametrized way (Herwig et al. 1997, 1999) rather suggest a *higher* C/He ratio; the intershell abundances which becomes visible after H-ingestion have C/He$\simeq 30\%$.

As is clear from the above discussion, an identification of the R CrB stars with one of the two scenarios is not straightforward. The situation is summarized in Table 7. Clearly there is an embarrasing richness of question marks for the various arguments. In particular, neither scenario is directly able to account for the observed abundances of the intermediate mass elements or the anti-correlation between the H and Fe abundances. However, considering that nebulosities have been detected surrounding the majority stars R CrB and UW Cen (Gillett et al. 1986; Pollacco et al. 1991) and that four members show presence of Li, it is tempting to associate the majority with final-flash objects. One might speculate that the DD scenario then is responsible for the minority. Whether it can produce the necessary intermediate mass elements and the s-elements remains to be shown.

A possible problem with identifying the majority with the FF scenario is posed by Sakurai's object. The star has some characteristics of both groups, as is also true for V854 Cen (Asplund et al. 1998). The two stars are distinctly overabundant in e.g. Na/Fe, like the minority, but are not distinguished by very high Si/Fe and S/Fe ratios, which otherwise normally define the minority members. Perhaps, all R CrB stars are FF objects but other processes introduce the extreme abundance ratios of the minority? However, there are some indication that the minority stars V3795 Sgr and VZ Sgr have higher C/He ratios than 1%. This is also true for V854 Cen (Asplund et al. 1998) and Sakurai's object (Asplund et al. 1999); the last minority star V CrA

is unfortunately too cool to allow an estimate. Such C/He ratios would be in better agreement with theoretical expectations of the FF event.

Unfortunately not much guidance can be obtained from a comparison with the EHe stars and the three hot R CrB stars. It is clear that the EHe and the R CrB stars resemble each other in general, though there are significant differences for certain elements, most notably for N and Ca and perhaps also Ni. It still seems plausible that the two classes share a common evolutionary background. However, the situation for the hot R CrB stars are far more confusing. DY Cen seems to be an extreme member of the minority group. V348 Sgr has a C/He ratio of 45%, which is more representative of the Wolf-Rayet central stars and the PG1159 stars (Leuenhagen & Hamann 1994). MV Sgr on the other hand has a very low C/He ratio of $1.8 \cdot 10^{-4}$ and thus more similar to the two peculiar EHe stars V652 Her and HD 144941 (Jeffery 1996). Both V348 Sgr and MV Sgr are also in other respects dissimilar to the R CrB stars in terms of chemical composition. Here, we must therefore refrain from suggesting particular evolutionary links between all the different groups of H-deficient stars.

7. Conclusions and challenges

Our attempts to decide what sequence of events that may turn stars into R CrB stars have reached only preliminary conclusions. This is partly due to intrinsic problems in our analysis, but more so due to the lack of detailed predictions of the nuclear processing and dredge-up in the different formation scenarios suggested. Furthermore, the knowledge about processes that could modify the chemical compositions of these stars during their evolution is insufficient. We find it astonishing that, in spite of considerable discussion on the origin of R CrB stars, very few models with predictions of abundances have been produced. Among the most urgent needs are studies of the resulting C/He ratios, of Li-production and carbon isotopic ratios, and of the possible production of intermediate elements during a final He-shell flash. For the merger scenario again the production of intermediate elements needs further exploration, as well as of Li and s-elements. Studies of dust formation and chemical processes in H-deficient, C-rich environments should also be undertaken, before more safe conclusions may be drawn concerning the role of dust-gas separation. To improve the chemical analysis non-LTE calculations should be performed for key elements like N, O, Si, S and Fe.

A significant result of the present study is the discovery of the intrinsic inconsistency in our analysis between the input and derived carbon abundances, a discrepancy which amounts to on average 0.6 dex. This quite significant "carbon problem" has not been resolved here. Its regularity indicates a general solution, not very much dependent on individual stellar parameters. Among the various explanations discussed we find the hypothesis of severe departures from standard "classical" model atmospheres or systematic errors in the current gf-values for C I most probable. The phenomenon should be explored further with semi-empirical model atmospheres. Also, spectra of

(H-rich) F supergiants should be studied in attempts to trace similar effects.

On the basis of the present knowledge of the consequences of the two proposed formation scenarios, as well as of dust-gas separation, no single scenario is able to explain even the majority group. This may be because the present preliminary understanding of the scenarios is incomplete or erroneous. Even as probable, however, seems the possibility that there is something fundamental that we do not understand concerning these enigmatic stars.

References

Acker A., Jaschek M., Gleizes F., 1982, A&AS 48, 363

Alcock C., Allsman R.A., Alves D.R., et al., 1996, ApJ 470, 583

Alexander J.B., Andrews P.J., Catchpole R.M., et al., 1972, MNRAS 158, 308

Asplund M., 1998, A&A 330, 641

Asplund M., Gustafsson B., 1996, In: Jeffery C.S., Heber U. (eds.) Hydrogen-deficient stars. ASP conf. series vol. 96, p. 39

Asplund M., Ryde N.A.E., 1996, In: Jeffery C.S., Heber U. (eds.) Hydrogen-deficient stars. ASP conf. series vol. 96, p. 57

Asplund M., Gustafsson B., Kiselman D., Eriksson K., 1997a, A&A 318, 521

Asplund M., Gustafsson B., Lambert D.L., Rao N.K., 1997b, A&A 321, L17

Asplund M., Gustafsson B., Rao N.K., Lambert D.L., 1998, A&A 332, 651

Asplund M., Lambert D.L., Kipper T., Pollacco D., Shetrone M.D., 1999, A&A 343, 507

Bell R.A., Gustafsson B., 1989, MNRAS 236, 653

Boyarchuk A.A., Hubeny I., Kubat J., et al., 1988, Afz 28, 343

Cameron A.G.W., Fowler W.A., 1971, ApJ 164, 111

Clayton D.D., 1968, Principles of stellar evolution and nucleosynthesis. McGraw-Hill, New York

Clayton G.C., 1996, PASP 108, 225

Clayton G.C., Whitney B.A., Stanford S.A., et al., 1992, ApJ 384, L19

Cottrell P.C., Lambert D.L., 1982, ApJ 432, 785

Drilling J.S., Schönberner D., Heber U., Lynas-Gray A.E., 1984, ApJ 278, 224

Drilling J.S., Jeffery C.S., Heber U., 1998, A&A 329, 1019

Edvardsson B., Andersen J., Gustafsson B., et al., 1993, A&A 275, 101

Fujimoto M.Y., 1977, PASJ 29, 331

Gillett F.C., Backman D.E., Beichman C., Neugebauer G., 1986, ApJ 310, 842

Glass I.S., Lawson W.A., Laney C.D., 1994, MNRAS 270, 347

Gonzalez G., Lambert D.L., Wallerstein G., et al., 1998, ApJS 114, 133

Gratton R.G., Carretta E., Eriksson K., Gustafsson B., 1999, A&A, in press

Grevesse N., Sauval A.J., 1998, In: Frölich C., Huber M.C.E., Solanki S.K., von Steiger R. (eds) Solar composition and its evolution – from core to corona. Kluwer, Dordrecht, p. 161

Gustafsson B., Asplund M., 1996, In: Jeffery C.S., Heber U. (eds.) Hydrogen-deficient stars. ASP conf. series vol. 96, p. 27

Gustafsson B., Bell R.A., Eriksson K., Nordlund Å., 1975, A&A 42, 407

Han Z., Podsiadlowski P., Eggleton P.P., 1994, MNRAS 270, 121

Hashimoto M., Hanawa T., Sugimoto D., 1983, PASJ 35, 1

Heber U., 1986, In: Hunger K., Schönberner D., Rao N.K. (eds.) Hydrogen-deficient stars and related objects. IAU coll. 87, Reidel, Dordrecht, p. 33

Herwig F., Blöcker T., Schönberner D., El Eid M., 1997, A&A 324, L81

Herwig F., Blöcker T., Langer N., Driebe T., 1999, A&A 349, L5

Hibbert A., Biémont E., Godefroid M., Vaeck N., 1993, A&AS 99, 179

Huber K.P., Herzberg G., 1979, Molecular spectra and molecular structure. Vol. 4, Constants of diatomic molecules. Van Nostrand Reinhold, New York

Hunger K., Schönberner D., Steenbock W., 1982, A&A 107, 93

Iben I. Jr., 1990, ApJ 353, 215

Iben I. Jr., MacDonald J., 1995. In: Koester D., Werner K. (eds.) White dwarfs. Springer, Berlin, p. 48

Iben I. Jr., Tutukov A.V., Yungelson L.R., 1996, ApJ 456, 750

Jeffery C.S., 1996, In: Jeffery C.S., Heber U. (eds.) Hydrogen-deficient stars. ASP conf. series vol. 96, p. 152

Jeffery C.S., 1998, MNRAS 294, 391

Jeffery C.S., Heber U., 1993, A&A 270, 167

Jeffery C.S., Hamill P.J., Harrison P.M., Jeffers S.V., 1998, A&A 340, 476

Jenkins E.B., 1987, In: Hollenbach D.J., Thronson H.A. Jr. (eds.) Interstellar processes. Reidel, Dordrecht, p. 533

Kipper T., Klochkova V.G., 1997, A&A 324, L65

Kurucz R.L., Peytremann E., 1975, SAO special report 362 (KP)

Lambert D.L., 1996, In: Jeffery C.S., Heber U. (eds.) Hydrogen-deficient stars. ASP conf. series vol. 96, p. 443

Lambert D.L., Rao N.K., 1994, JA&A 15, 47

Lambert D.L., Rao N.K., Giridhar S., 1990, JA&A 11, 475

Lambert D.L., Heath J.E., Lemke M., Drake J., 1996, ApJS 103, 183

Leuenhagen U., Hamann W.-R., 1994, A&A 283, 567

Lodders K., Fegley B.Jr., 1995, Meteoritics 30, 661

Luo D., Pradhan A.K., 1989, J. Phys. B. 22, 3377

Malaney R.A., 1987a, ApJ 321, 832

Malaney, R.A., 1987b, Ap&SS 137, 251

Mihalas D., 1978, Stellar atmospheres. W.H. Freeman and Company, San Francisco

Paczyński B., 1971, Acta Astron. 21, 417

Peach G., 1970, Mem. R. Astron. Soc. 73, 1

Plez B., Brett J.M., Nordlund Å., 1992, A&A 256, 551

Politano M., Starrfield S., Truran J.W., et al., 1995, ApJ 448, 807

Pollacco D.L., Hill P.W., Houziaux L., Manfroid J., 1991, MNRAS 248, 1P

Pollard K.R., Cottrell P.L., Lawson W.A., 1994, MNRAS 268, 544

Rao N.K., Lambert D.L., 1993, PASP 105, 574

Rao N.K., Lambert D.L., 1996, In: Jeffery C.S., Heber U. (eds.) Hydrogen-deficient stars. ASP conf. series vol. 96, p. 43

Rao N.K., Lambert D.L., 1997, MNRAS 284, 489

Rao, N.K., Nandy K., Bappu M.K.V., 1981, MNRAS 195, 71P

Rao N.K., Lambert D.L., Adams M.T., et al., 1999, MNRAS, in press

Renzini A., 1979, In: Westerlund B.E. (ed.) Stars and star systems. Reidel, Dordrecht, p. 155

Renzini A., 1990, In: Cacciari C., Clementini G. (eds.) Confrontation between stellar pulsation and evolution. ASP conf. series vol. 11, p. 549

Savage B.D., Sembach K.R., 1996, ARA&A 34, 279

Schönberner D., 1975, A&A 44, 383

Schönberner D., 1996, In: Jeffery C.S., Heber U. (eds.) Hydrogen-deficient stars. ASP conf. series vol. 96, p. 433

Seaton M.J., Yan Y., Mihalas D., Pradhan A.K., 1994, MNRAS 266, 805

Stürenburg S., Holweger H., 1990, A&A 237, 125

Takeda Y., Takada-Hidai M., 1995, PASJ 47, 169

Thorne K.S., Żytkow A.N., 1975, ApJ 199, L19

Unsöld A., 1955, Physik der Sternatmosphären. Springer-Verlag, Berlin

Vanture A.D., Zucker D., Wallerstein G., 1999, ApJ 514, 932

Venn K.A., 1996, PASP 108, 209

Walker H.J., 1986, In: Hunger K., Schönberner D., Rao N.K. (eds.) Hydrogen-deficient stars and related objects. Reidel, Dordrecht, p. 407

Webbink R.F., 1984, ApJ 277, 355

Weiss A., 1987, A&A 185, 178

Wheeler J.C., Sneden C., Truran J.W. Jr., 1989, ARA&A 27, 279

Wiese W.L., Smith M.W., Miles B.M., 1969, Atomic Transition Probabilities. NSRDS-NBS 22